

MICROWAVE BEAMFORMER RECEIVER FRONT END



By

Muhammad Saad Zia

Muhammad Faizan

Hassaan Ahmad

Jawad Ullah

Project Supervisor: Dr. Farooq Ahmad Bhatti

Submitted to the Faculty of Electrical Engineering, Military College of Signals,
National University of Sciences and Technology, Rawalpindi in partial fulfillment for
the requirements of a B.E Degree in Telecommunication Engineering

JUNE 2012

ABSTRACT

MICROWAVE BEAMFORMER RECEIVER FRONT END

Telecommunication industry has always competed against limited resources and increasing number of users. Smart Antennas are now becoming attractive tool as they reduce the interference and maximize the bandwidth utilization. Smart antennas have, in recent times, received considerable attention for their use in communications, electronic surveillance and electronic countermeasures where it is advantageous to have a single antenna that can dynamically steer the beam to the desired angle to transmit or receive the signals.

The report includes the design and analysis of a Microwave Sampling Beamformer with beam steering capability. A Microwave Sampling Beamformer consisting of four patch antennas has been developed and tested. The project consists of RF hardware, microwave hardware and control circuitry. Agilent ADS software has been used as a design tool. PIN diodes have been used as phase shifters in the design. A novel phase shifting switch design has been implemented in the structure. The control circuitry consists of four pulse generators driven by the same oscillator. PIN diode drivers have been designed to provide appropriate biasing conditions and to ensure impedance matching between the pulse generators and the diodes. The microwave part includes RF amplifier, frequency down-converting mixer, Intermediate Frequency amplifier and low pass filter. The phase shift for each of the four patch antennas is controlled through the time delay of the corresponding pulse train.

The measured results show that the structure is capable of steering the beam in the range of ± 45 degrees. The structure has been designed and tested to operate at a frequency of 5.8 GHz.

CERTIFICATE OF CORRECTNESS AND APPROVAL

It is certified that the work contained in the thesis titled “Microwave Beamformer Receiver Front End”, carried out by Muhammad Saad Zia, Muhammad Faizan, Hassaan Ahmad and Jawad Ullah under the supervision of Dr. Farooq Ahmad Bhatti in partial fulfillment of the degree of Bachelor of Telecommunication Engineering, is correct and approved.

Approved By

Dr. Farooq Ahmad Bhatti
Project Supervisor
Military College of Signals, NUST



DEDICATION

To Almighty Allah, for Whose greatness we do not have enough words,

To our parents and friends, whose undaunted support, made a work of this magnitude

possible

ACKNOWLEDGEMENTS

First of all, we praise Allah Almighty, who gave us strength to undertake this project and to complete it in a timely and efficient manner.

We wish to express our gratitude to our supervisor; Dr. Farooq Ahmad Bhatti, from the Faculty of Department of Electrical Engineering, Military College of Signals, National University of Sciences and Technology, for his continuous support and supervision during the course of the project. His persistent guidance is certainly commendable.

We would specially like to thank Mr. Zahid Yaqoob Malik. It would not have been possible to complete the project on time without his technical and moral support.

We would also like to acknowledge the struggle of our parents for our well being and education. They have done endless efforts to make us stand out. We would designate our success to them.

At the end, we would like to thank Mr. Ali from RIMMS, NUST for his help in antenna measurements and results.

TABLE OF CONTENTS

CHAPTER 1: INTRODUCTION.....	1
1.1. Background.....	1
1.2.Literature Review.....	2
1.2.1.Smart Antenna	2
1.2.2.Beamforming	2
1.3. Beamforming Techniques.....	3
1.4. Methodology.....	4
CHAPTER2: ANTENNA DESIGN.....	6
2.1. Microstrip Patch Antennas.....	6
2.2. Rectangular Patch	7
2.2.1.Transmission Line Analysis.....	7
2.2.2. Concept of Radiation in Patch Antenna	8
2.3. Feeding Methods.....	9
2.4. Substrate Properties	11
2.5. Antenna Design.....	12
2.6. Antenna Model Simulation.....	15
2.7. Antenna Array.....	19
2.8. Design of Antenna Array in ADS.....	19
CHAPTER 3: PHASE SHIFTING SWITCH	22
3.1. Always-Matched Switch.....	22
3.2. Novel Phase Shifting Switch.....	22
3.3. Design of the Switch in ADS.....	22
3.3.1. First State	27
3.3.2. Second State.....	27
CHAPTER 4: WILKINSON POWER COMBINER	29
4.1 Power Dividers and Combiners	29
4.2 Types of Dividers.....	31
4.2.1 Junction / T-line	31
4.2.2 Lossless Dividers	32
4.2.3 Resistive Dividers	34
4.2.4 Wilkinson Power Divider.....	34
CHAPTER 5: POWER COMBINER AND FEED NETWORK DESIGN	37

5.1 Design of Wilkinson Power Combiner in ADS	37
5.2 Feed Network Design	39
CHAPTER 6: MICROWAVE DOWN-CONVERTER	41
6.1. Overview	41
6.2. Low Noise Amplifier	42
6.2.1. Noise Figure and Gain	42
6.2.2. Linearity of LNA	44
6.2.3. Bandwidth and Flat Gain:	44
6.2.4. Voltage Standing Wave ratio	44
6.2.5. MGA-86576 LNA IC.....	45
6.3. Frequency Mixer.....	45
6.3.1. Mixer Properties.....	47
6.3.2. Types of Mixers	50
6.3.2.1.Single Device (diode) Mixer.....	50
6.3.2.2. Balanced Mixers	50
6.3.3. SIM 14+ Mixer IC	53
6.4. IF – Amplifier	54
6.5. Design of the Downconverter	54
6.6. Results of the Downconverter.....	56
CHAPTER 7: MICROWAVE HOUSING	60
CHAPTER 8: CONTROL CIRCUITRY	64
8.1. Overview	64
8.2. Control Signals.....	65
8.3. PIN Diode Driver	68
CHAPTER 9: BEAMFORMING / BEAM STEERING RESULTS	69
CONCLUSION	71
APPENDICES	72
APPENDIX A	73
APPENDIX B	74
BIBLIOGRAPHY	75

LIST OF TABLES

<i>Table no.</i>	<i>Page no.</i>
4-1: Insertion Loss vs. Output Ports	29
4-2: Summary of Dividers	36
5-1: Design Parameters for Wilkinson Power Divider	37
6-1: The Input / Output Transfer Characteristics of a 4-Port Hybrid Junction.....	52
6-2: Electrical Specifications of the SIM 14+ Mixer IC.....	53
6-3: Overall Gain vs. the LO Drive Power Relation.....	56

LIST OF FIGURES

<i>Figure no.</i>	<i>Page no.</i>
1-1: Microwave Beamformer Receiver Modules.....	4
1-2: Block Diagram of Microwave Beamformer Receiver.....	5
2-1: Fringing Fields in Rectangular Patch	7
2-2: Basic Microstrip Patch radiation	9
2-3: Probe Feed	10
2-4: Aperture-Coupled Feed	11
2-5: Proximity-Coupled Feed.....	11
2-6: Denotation of Dimensions of Rectangular patch	13
2-7: Design of the Patch Antenna in ADS	15
2-8: S_{11} Parameter of the Patch Antenna	16
2-9: Gain of a Single Element Patch Antenna	16
2-10: Directivity of a Single Element Patch Antenna.....	17
2-11: Efficiency of Patch Antenna.....	18
2-12: Power Radiated and Radiation Pattern	18
2-13: Coupling between Antenna Elements.....	19
2-14: Complete Array Design.....	20
2-15: Gain of Array.....	21
3-1: First Design for Always-Matched Switch	23
3-2: Second Design for Always-Matched Switch.....	24
3-3: Novel Phase Shifting Switch	25
3-4: Pulse Train.....	25
3-5: Switch Design in ADS	26
3-6: Result of State 1.....	27
3-7: Result of State 2.....	28
4-1: 3-Port Power Divider.....	30
4-2: T-Junction.....	32
4-3: Lossless Divider	32
4-4: Matching of Lossless Divider.....	33
4-5: “Delta” and “Wye” Configurations of Resistive Divider.....	34
4-6: Three-Port Wilkinson Power Divider.....	35
5-1: Wilkinson Power Combiner Layout in ADS.....	37
5-2: Insertion Loss of WPC	38

5-3: Return Loss of WPC.....	38
5-4: Port to Port Isolation.....	39
5-5: Layout of Complete Feed Network in ADS	40
5-6: Return Loss of Complete Feed Network.....	40
6-1: Block Diagram of Down-Converter Part.....	41
6-2: Mixer Compression	48
6-3: Equivalent Circuit of a Single Diode Mixer.....	50
6-4: 4-port Hybrid Junction	51
6-5: Mixer Constructed from a 4-Port Hybrid Junction.....	52
6-6: Construction of a Double Balanced Mixer from 4-Port Hybrid Junction	52
6-7: Electrical Schematics of SIM 14+	53
6-8: Schematics of the Downconverter.....	54
6-9: Layout of the Downconverter PCB	55
6-10: Fabricated Downconverter PCB.....	55
6-11: IF Output	57
6-12: RF VSWR.....	57
6-13: LO VSWR	58
6-14: Setup for Measuring VSWR.....	58
6-15: Setup for Measuring IF.....	59
7-1: Design of Microwave Housing in AutoCAD	62
7-2: Isometric View of Microwave Housing	62
7-3: Fabricated Microwave Housing	63
8-1: Forward Biased Model of PIN Diode.....	64
8-2: Reverse Biased Model of PIN Diode	65
8-3: Block Diagram of Control Circuitry.....	66
8-4: Schematic of Pulse Generator and Time Delay Circuit.....	67
8-5: Output of Pulse Generator and Time Delay Circuit	67
8-6: Schematic of PIN Diode Driver	68
9-1: Complete Beamformer Structure.....	69
9-2: Beam at 0 Degrees.....	69
9-3: Beam Steered at 15 Degrees.....	70
9-4: Beam Steered at -15 Degrees	70
9-5: Beam Steered at 40 Degrees.....	71

LIST OF ABBREVIATIONS

ADC	Analog to Digital Converter
ADS	Advanced Design System
CW	Continuous Wave
dB	Deci Bels
DC	Direct Current
DIP	Dual In-line Package
DOA	Direction Of Arrival
GHz	Giga Hertz
IC	Integrated Circuit
IF	Intermediate Frequency
LO	Local Oscillator
LNA	Low Noise Amplifier
LPF	Low Pass Filter
MHz	Mega Hertz
MMIC	Monolithic Microwave Integrated Circuit
NF	Noise figure
PCB	Printed Circuit Board
PIN	Positive-Intrinsic-Negative

RF	Radio Frequency
S-parameter	Scattering parameter
SMA	SubMiniature version A
VSWR	Voltage Standing Wave Ratio

INTRODUCTION

1.1. Background

Beam-forming is a technique that employs Smart antenna technology and offers a considerably better solution to decrease interference levels and improve the system capacity. With this technology, each user's signal is transmitted and received by the base station only in the direction of that particular user. This radically decreases the overall interference in the system and saves the transmitted power. A smart antenna system makes use of an array of antennas that work together to direct different transmission/reception beams toward each user in the system. This technique of transmission and reception is called beam-forming and is made possible through smart (advanced) signal processing at the baseband level.

In beam-forming, each user's signal is multiplied with complex weights that adjust the magnitude and phase of the signal to and from each antenna. This causes the output from the array of antennas to form a transmit/receive beam in the desired direction and decreases the output in other directions.

A major challenge in deploying beam-forming in commercial wireless communications is the high implementation cost. Microwave beam-forming (MBF) is a low complexity alternative due to using only one radio frequency (RF) down-conversion and analog to digital converter (ADC). The downconverter and the Analog to Digital Converter are required to make the received signal compatible for further processing by a Digital Signal Processor (DSP).

1.2. Literature Review

This section states the background study, motivation and need of the product developed as a result of this research. The detailed objectives and the thesis outline are also presented to give an overview of the project.

1.2.1. Smart Antenna

Smart antenna systems are generally known as smart antennas, but in reality antennas are not smart by themselves. Actually, it is the digital signal processing capability, along with the antennas, which make the system smart. A smart antenna system comprises of an antenna capable of Beam-forming and Digital Signal Processing at the back end which is actually an algorithm for Direction of Arrival (DOA) estimation[1]. Electrical smart antenna consists of two or more antennas, a digital signal processor Based on the time delays due to the impinging signals onto the antenna elements. The digital signal processor computes the direction-of-arrival (DOA) of the signal-of-interest (SOI). Then it adjusts the excitations (gains and phases of the signals) to produce a radiation pattern that focuses on the SOI while tuning out any interferers or signals-not-of-interest (SNOI) i.e. Beam-forming.

1.2.2. Beamforming

Beam-forming is a signal processing technique that is used in sensor arrays to receive or to transmit a signal in a particular direction. This phenomenon is achieved using an array of antennas and the elements in the array are combined in such a way that constructive interference is observed by the signals at some particular angles while at other angles, destructive interference is observed [1]. Beamforming is a technique that can be employed at both the transmitter and receiver end to obtain spatial selectivity.

Beamforming has found various different applications. It can be used for both radio and sound waves. Beamforming is employed in Phased Array RADARs, SONAR, seismology, wireless communication, radio astronomy. Adaptive Beamforming is another technology that is used to detect an estimate of the desired signal at the output of a sensor array by means of techniques such as data adaptive spatial filtering and interference rejection.

1.3. Beamforming Techniques

Deploying beamforming in commercial wireless applications demands reduction in implementation cost and complexity. Some techniques of Beam forming are Digital Beamforming (DBF), Spatially Multiplexing of Local Elements (SMILE), Hybrid analog DBF, Microwave Beamforming (MBF) [2].

Digital beamforming (DBF) allows using sophisticated signal processing operations on the array signals. However, one full receiver including RF down-conversion, low-pass filter (LPF), and analog-to-digital converter (ADC) should be used after each antenna element, which makes this structure very complex and costly. In addition, multiple signals are transferred to the processor in parallel which limits the data throughput due to the speed bottleneck limitation of the current digital signal processor (DSP) technology.

The technique of spatially multiplexing of local elements (SMILE), in which the antenna array signals are transferred to the processor sequentially in time multiplex fashion to implement beamforming in the digital domain. This technique uses one RF down conversion branch to lower the complexity. Hybrid analog-DBF is a technique in which Beamforming is performed in the analog IF domain to overcome the speed bottleneck of the processor.

Microwave beamforming (MBF) is an attractive alternative due to using one RF down-conversion and ADC branches. Moreover, because only one signal is transferred to the processor higher throughput is possible. On the other hand, having a single receiver in the MBF structure limits its signal processing capability [2].

1.4. Methodology

In this project, there is an array of four patch antennas which is used to receive the signal. Then the combined signal of these four antennas is used to form a beam. PIN diodes are used as phase shifters to shift the beam at various angles. Then there is the frequency down-converting part consisting of RF amplifier, mixer, IF amplifier and low pass filter. The output frequency of the down-converting part is 60 MHz. The 60 MHz signal is compatible for analog to digital conversion through an ADC. The figure 1-1 below shows the different modules of the project.

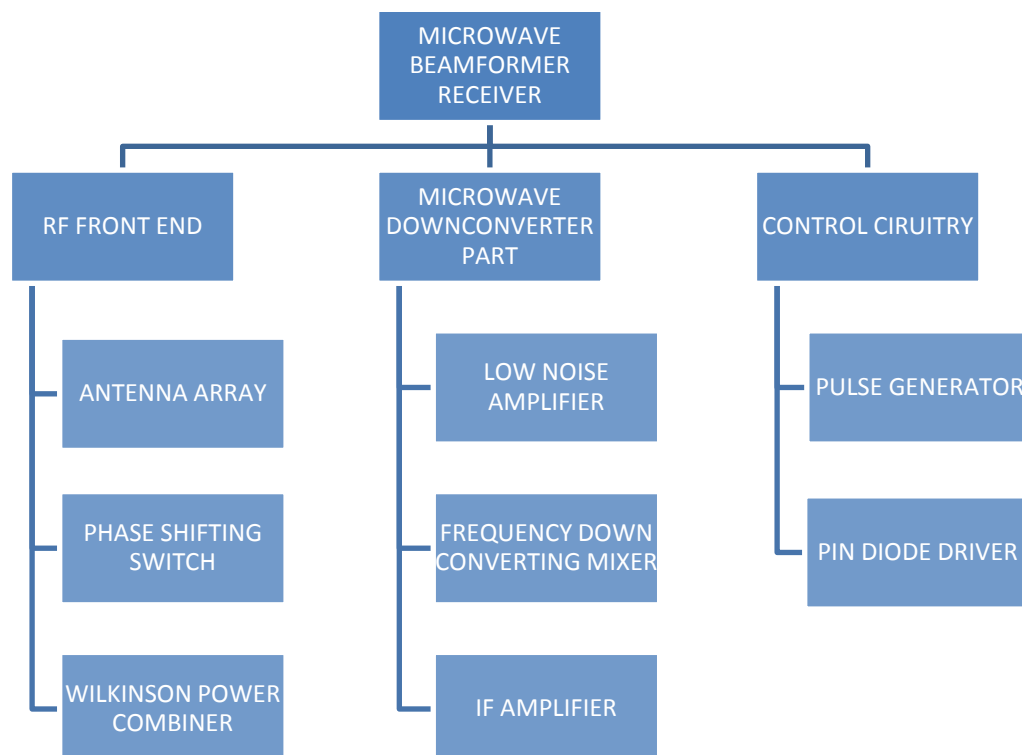


Figure 1-1: Microwave Beamformer Receiver Modules

The patch antennas are designed and optimized at a frequency of 5.8 GHz. Agilent ADS is used as a design tool. The antennas are followed by 4 phase shifting switches. These switches employ PIN diodes for fast switching.

The Block Diagram of the complete system is given in the figure 1-2.

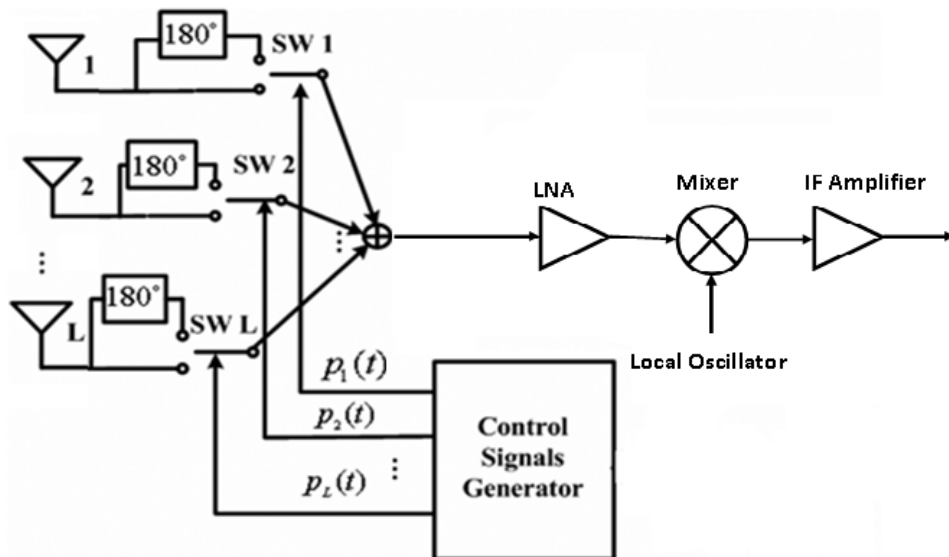


Figure 1-2: Block Diagram of Microwave Beamformer Receiver

ANTENNA DESIGN

2.1. Microstrip Patch Antennas

Microstrip patch antennas are low profile antennas which are conformable to planar as well as non planar surfaces and are simple and economical to manufacture. Selection of the particular patch shape and mode makes the patch antennas very versatile in terms of resonant frequency, polarization, pattern and impedance [3].

Some of the major operational drawbacks of microstrip patch antennas are that they have low efficiency, they are low profile in nature, they have high Quality factor which is sometimes more than 100, poor polarization purity, poor scan performance, spurious feed radiation and very narrow frequency bandwidth. However there are methods, such as increasing the height of the substrate that can be used to increase the efficiency and bandwidth. On the other hand, as the height of the substrate increases, surface waves are generated which generally are not desired because they extract the power from the total available power for direct radiation (space waves). The surface waves are such that they travel within the substrate and they are scattered at bends and surface discontinuities, such as the truncation of the dielectric and ground planes [3].

Microstrip patch antennas consist of a very thin metallic strip which is placed a small fraction of a wavelength above the ground plane. The patch and the ground plane are separated by a dielectric sheet, known as the substrate. The microstrip patch antenna is also called a broadside radiator because it is designed in such a way so that its pattern maximum is normal to the patch. The length of the element is usually:

$$\lambda_0 / 3 < L < \lambda_0 / 2$$

2.2. Rectangular Patch

The rectangular patch is the most commonly used arrangement for patch antennas. It can be easily modeled and analyzed using different models such as the transmission line model and the cavity model which are most perfect for thin substrates.

In this report, only the transmission line model analysis of the patch antenna is discussed.

2.2.1. Transmission Line Analysis

Using the transmission line model, the rectangular patch antenna can be represented by two slots, separated by a low impedance transmission line.

Since the dimensions of the patch antenna are finite along the length and width, the fields at the edges undergo fringing [4]. This is shown in the figure 2-1.

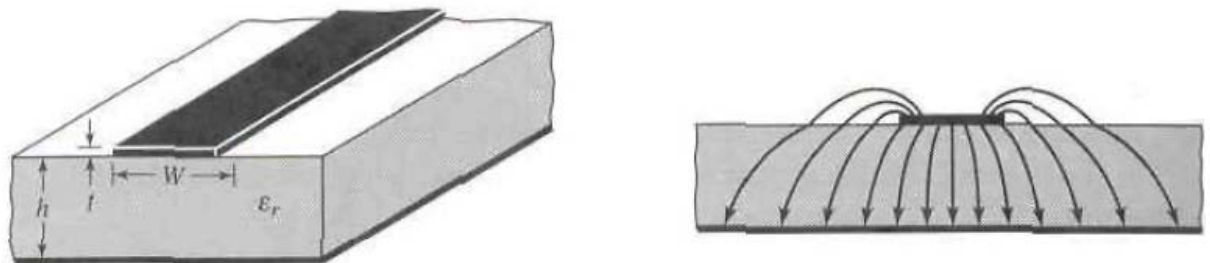


Figure 2-1: Fringing Fields in Rectangular Patch

The amount of fringing is a function of the dimensions of the patch antenna and the height of the substrate. For the E-plane, fringing is a function of the ratio of the length of the patch L to the height of the substrate h and the dielectric constant of the substrate.

The two important and critical steps in designing the patch antenna were the definition of the patch dimensions and the feeding configuration. The patch dimensions have direct effect on the operating frequency and on the antenna gain. The difficulty to predict the dimensions of the patch antenna accurately, is related to the fringing fields together with the small size of the ground plane used [4].

The antenna feeding should be designed carefully since it must provide a correct impedance matching. At high-signal frequencies it is essential to design a feeding line with specific characteristic impedance. Also, that line must be connected in a point of the antenna where the input impedance is the same than the feed-line characteristic impedance. The patch antenna was fed with a microstrip line connected to a point inside the patch where the input impedance is 50Ω .

2.2.2. Concept of Radiation in Patch Antenna

In order to have complete and clear understanding of working of this antenna, it is important to have the concept of radiation in a single patch antenna.

The substrate is clad with two conductive layers. The resonant frequency depends upon dimensions and substrate properties. The feed probe couples Electromagnetic Energy into the antenna structure. Lowest order mode is TE_{10} . The electric field is zero at the centre and the minimum and maximum continuously change side according to the instantaneous phase of the applied signal. It is due to these fringing fields that results in radiation of patch antenna [4]. Figure 2-2 shows the concept of radiation in patch antenna. The different feeding methods for the rectangular microstrip patch antenna and the design equations for the rectangular patch antenna are discussed later in the chapter. The design of a single antenna element and the antenna array in Agilent ADS is given at the end of this chapter.

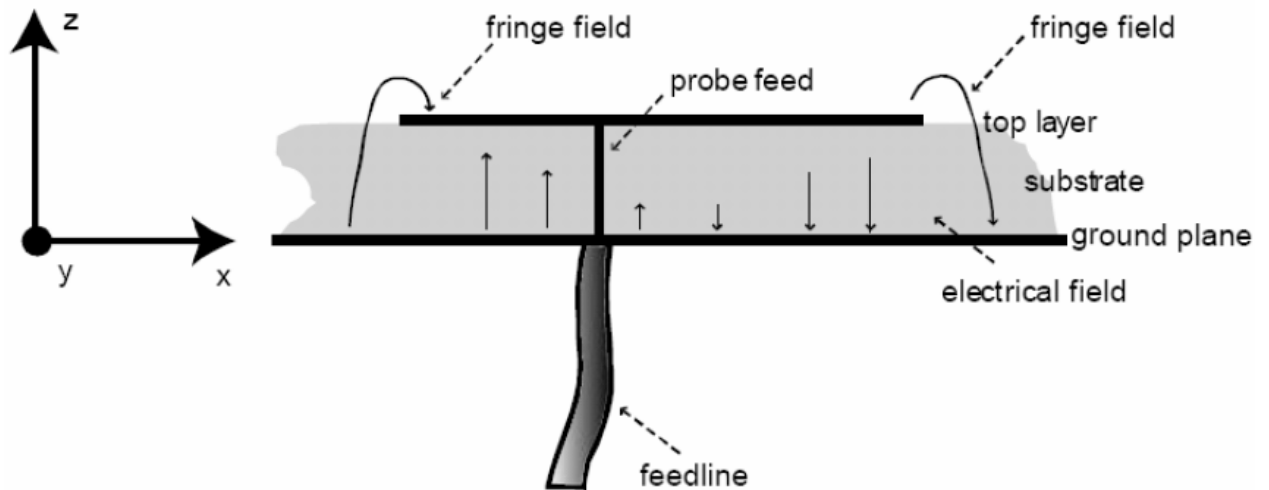


Figure 2-2: Basic Microstrip Patch Radiation

2.3. Feeding Methods

There are many configurations that can be used to feed microstrip antennas. The most popular are Microstrip line, Coaxial probe feed, Aperture coupling and Proximity coupling [4]. Each of these feeding methods is discussed in detail in the following paragraphs.

The microstrip feed line is also a conducting strip usually of much smaller width compared to the patch. The microstrip line feed is easy to fabricate, simple to match by controlling the inset position and quite simple to model. However, as the substrate thickness increases, surface waves and spurious feed radiation increase which for practical designs limit the bandwidth.

Coaxial line feeds where the inner conductor of the coax is attached to the radiation patch while the outer conductor is connected to the ground plane are also widely used. The coaxial probe feed is also easy to fabricate and match and it has low spurious radiation. However, it also has narrow bandwidth and it is more difficult to model specially for thick substrates [5]. Figure 2-3 shows the probe feed mechanism.

In the figure 2-3, a circular patch antenna is shown on a dielectric substrate with the coaxial connector connected towards the ground plane of the substrate. The coaxial connector is connected to the patch by means of a small probe. The patch antenna is excited by applying an excitation at the coaxial connector.

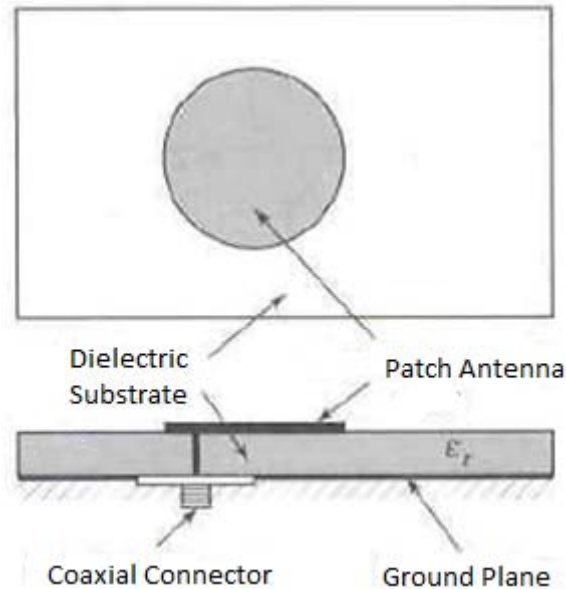


Figure 2-3: Probe Feed

The aperture coupling is the most complex of all four to fabricate and it also has narrow bandwidth. However, it is somewhat easier to model and has moderate spurious radiation. The aperture coupling comprises of two substrates separated by a ground plane. On the bottom side of the lower substrate, there is a microstrip line whose energy is coupled to the patch through a slot on the ground plane separating the two substrates. Typically a high dielectric material is used for the bottom substrate and thick low dielectric constant material for the top substrate. The ground plane between the substrates also isolates the feed from the radiating element and minimizes interference of spurious radiation for pattern formation and polarization purity [5]. Figure 2-4 shows the aperture coupled feed.

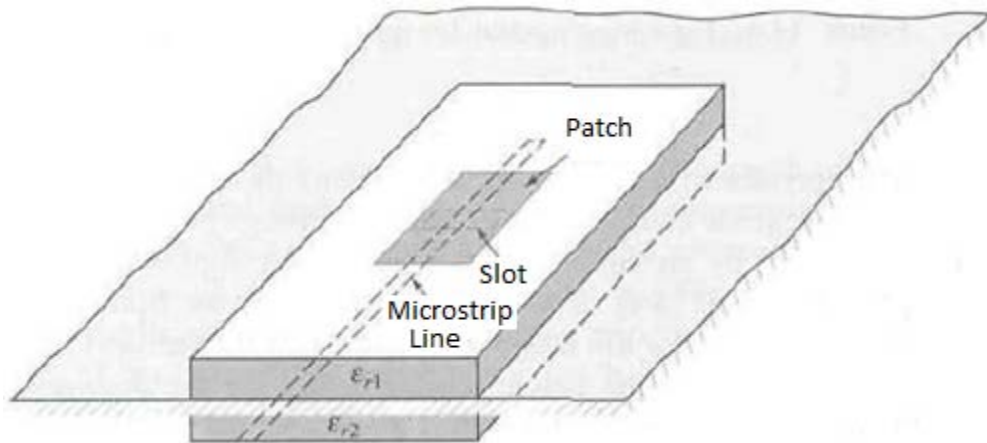


Figure 2-4: Aperture-Coupled Feed

The proximity coupling is same as aperture coupling but it has the largest bandwidth (as high as 13 percent), is somewhat easier to model and has low spurious radiation. However, its fabrication is somewhat more difficult. The length of the feeding stub and the width to line ratio of the patch can be used to control the match.

Figure 2-5 shows the proximity coupled feeding method.

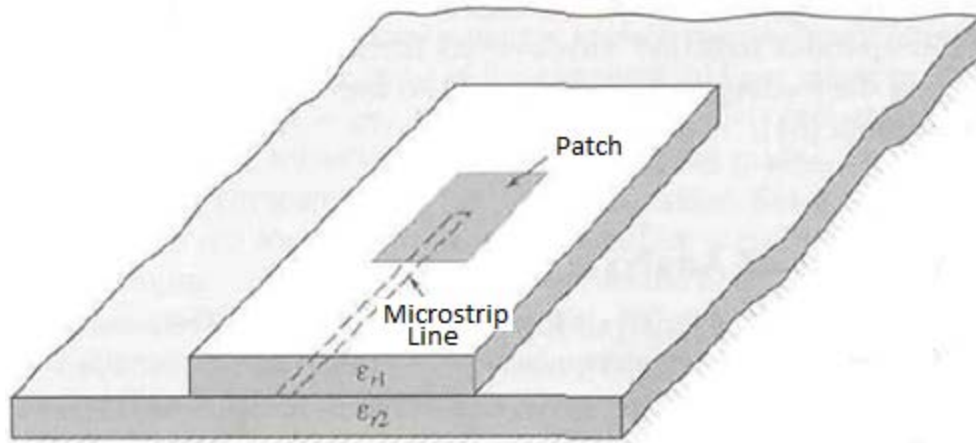


Figure 2-5: Proximity-Coupled Feed

2.4. Substrate Properties

There are various substrates that can be used for the design of microstrip antennas, and their dielectric constants are usually in the range of $2.2 \leq \epsilon_r \leq 12$ [5]. The ones

that are most desirable for good antenna performance are thick substrates whose dielectric constant is in the lower end of the range because they provide better efficiency, larger bandwidth, loosely bound fields for radiation into space, but at the cost of larger element size. Thin substrates with higher dielectric constants are enviable for microwave circuitry because they require tightly bound fields to minimize undesired radiation and coupling, and lead to smaller element sizes; however, as the losses increase, they are less efficient and have comparatively smaller bandwidths.

The substrate selected for this project was the Rogers RO-4350B because its dielectric constant $\epsilon_r = 3.66$ which is desirable for good performance as it is in the lower end of the range. Also the height of the substrate $h = 20$ mils, which is low and hence good for microwave circuitry of this project.

2.5. Antenna design

Three of the parameters were known before other calculations which were the dielectric constant of the substrate (ϵ_r), the resonant frequency (f_r) and the height (h) of the substrate. The substrate used is Rogers RO-4350B with dielectric constant $\epsilon_r = 3.66$ and height $h = 20$ mils (0.02 inch). The resonant frequency is $f_r = 5.8$ GHz.

Figure 2-6 shows the dimensions of the rectangular patch antenna.

The equations used for calculating the dimensions of the patch antenna are given after figure 2-6. Equations 2.1 through 2.6 were used to calculate the dimensions of the rectangular patch antenna at 5.8 GHz frequency. Using the results obtained through these equations, the antenna was designed in Agilent ADS software.

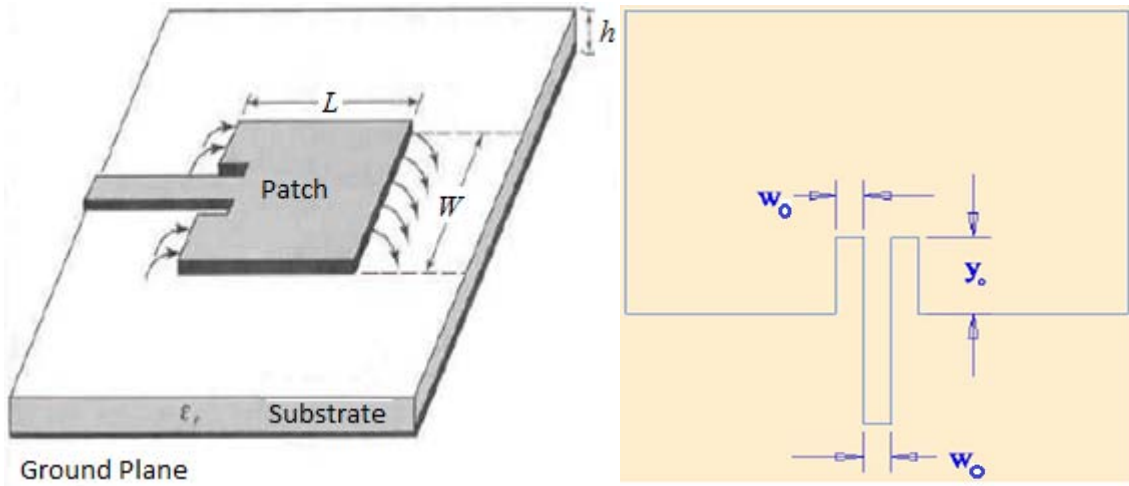


Figure 2-6: Denotation of Dimensions of Rectangular Patch

$$W = \frac{1}{2f_r \sqrt{\mu_0 \epsilon_0}} \sqrt{\frac{2}{\epsilon_r + 1}} = \frac{v_0}{2f_r} \sqrt{\frac{2}{\epsilon_r + 1}} \quad (2.1)$$

Where v_0 is the velocity of light in free space.

For $W/h > 1$, the effective dielectric constant ($\epsilon_{r\text{eff}}$) of the microstrip antenna is

then calculated by :

$$\epsilon_{\text{eff}} = \frac{\epsilon_r + 1}{2} + \frac{\epsilon_r - 1}{2} \left[1 + 12 \frac{h}{W} \right]^{-1/2} \quad (2.2)$$

Then the extended length (ΔL) is found by following formula:

$$\frac{\Delta L}{h} = 0.412 \frac{(\epsilon_{\text{eff}} + 0.3) \left(\frac{W}{h} + 0.264 \right)}{(\epsilon_{\text{eff}} - 0.258) \left(\frac{W}{h} + 0.8 \right)} \quad (2.3)$$

The actual length (L) of the patch is then found by:

$$L = \frac{1}{2f_r \sqrt{\epsilon_{eff}} \sqrt{\mu_0 \epsilon_0}} - 2\Delta L \quad (2.4)$$

The antenna is fed by an inset feed line. The width of the feed line (W_o) with characteristic impedance Z_c , where the required impedance of the line was $Z_c=50\Omega$, was calculated from:

$$Z_c = \frac{120\pi}{\sqrt{\epsilon_{reff}} \left[\frac{W_o}{h} + 1.393 + 0.667 \ln \left(\frac{W_o}{h} + 1.444 \right) \right]} ; \frac{W_o}{h} > 1 \quad (2.5)$$

The inset feed point (y_o) was then calculated by the formula:

$$y_o = 10^{-4} \left\{ \begin{array}{l} 0.001699\epsilon_r^7 + 0.13761\epsilon_r^6 - 6.1783\epsilon_r^5 + 93.187\epsilon_r^4 - 682.69\epsilon_r^3 + \\ 2561.9\epsilon_r^2 - 4043\epsilon_r + 6697 \end{array} \right. \quad (2 \leq \epsilon_r \leq 10) \quad \left. \right\} \frac{L}{2} \quad (2.6)$$

The length of the Microstrip feed line was kept equal to $\lambda_o/3$ and the width of the notches were also kept same as the width (W_o) of the feedline.

The results obtained using these formulae are:

Width (W) = 16.943 mm

Effective dielectric constant (ϵ_{eff}) = 3.472

Extended Incremental length (ΔL) = 2.38 mm

Length (L) = 13.402 mm

Width of feed line (W_o) = 1.147 mm

Inset Feed Point Distance (y_o) = 3.85 mm

2.6. Antenna Model Simulation

The antenna with the calculated dimensions was then designed in ADS software. It is depicted in figure 2-7 along with the results. A return loss of less than -31 dB is obtained at the resonant frequency. The return loss of a single antenna is shown in figure 2-8.

The antenna has been designed and simulated in momentum in Agilent ADS software.

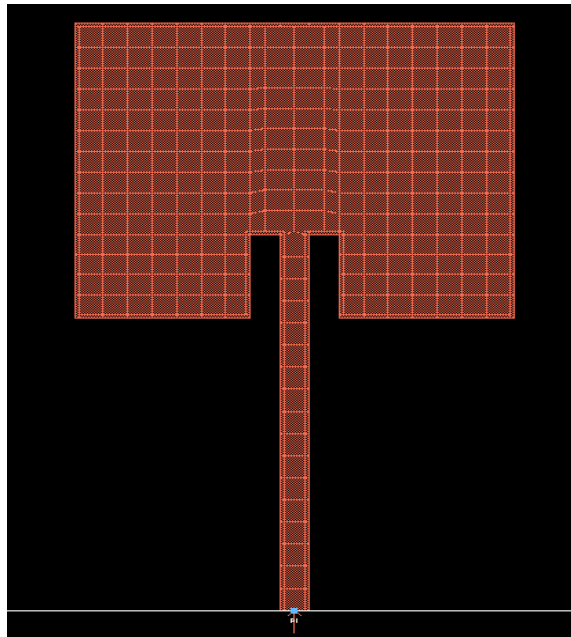


Figure 2-7: Design of the Patch Antenna in ADS

The reflection coefficient or the S_{11} parameter of the single element patch antenna is found to be -31 dB. The graph for the reflection coefficient is shown in figure 2-8. The reflection coefficient was obtained after simulating the antenna in Agilent ADS Momentum. An optimal reflection coefficient for the antennas is below -10 dB. A reflection coefficient of -31 dB indicates that the antenna is optimized at the resonating frequency of 5.8 GHz and the reflections are minimum at this frequency. Most of the power that is input to the antenna is converted into electromagnetic radiations.

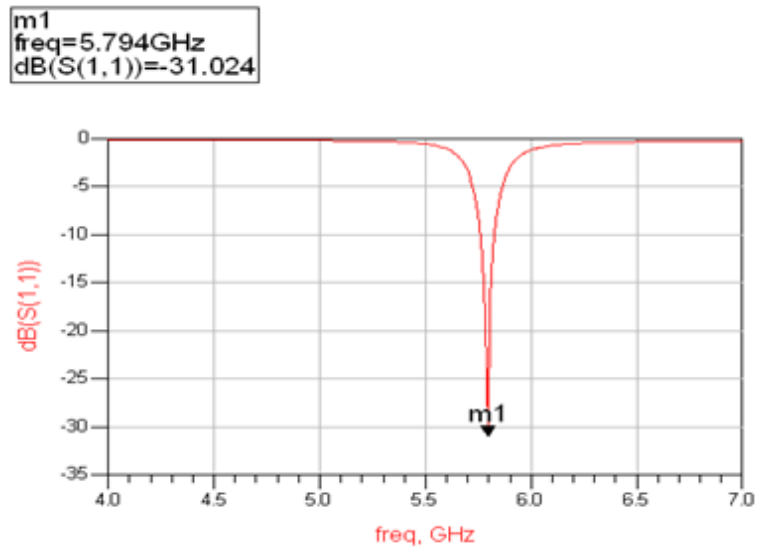


Figure 2-8: S_{11} parameter of the Patch Antenna

Patch antennas are low profile antennas whose gains are not very large. The gain of an antenna is defined as: “the ratio of the intensity, in a given direction, to the radiation intensity that would be obtained if the power accepted by the antenna were radiated isotropically” [3]. The optimum gain of a patch antenna lies within the range of 6 to 8 dB. Figure 2-9 shows the gain of a single element patch to be 7.2 dB.

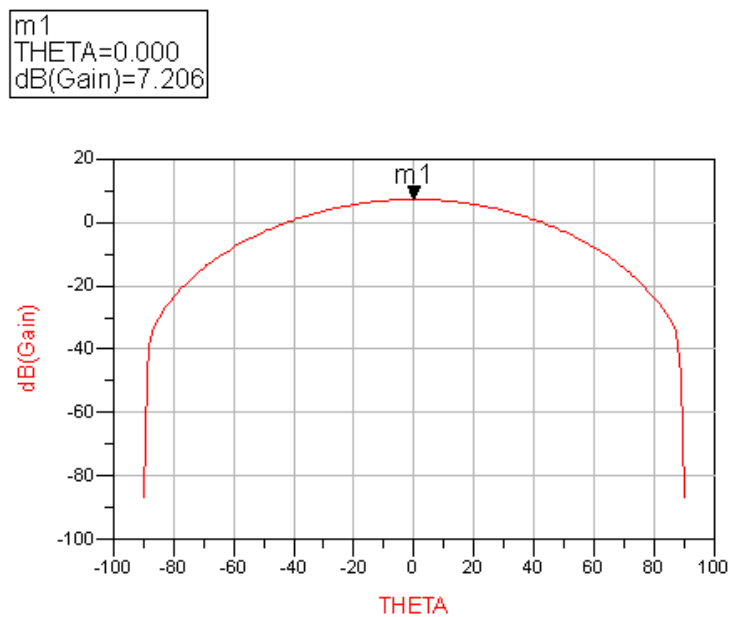


Figure 2-9: Gain of a Single Element Patch Antenna

The directivity of an antenna is defined as: “The ratio of the radiation intensity in a given direction from the antenna to the radiation intensity averaged over all directions” [3].

The directivity of the antenna designed at a frequency of 5.8 GHz is found out to be 13.38 dB. The graph of directivity is shown in figure 2-10.

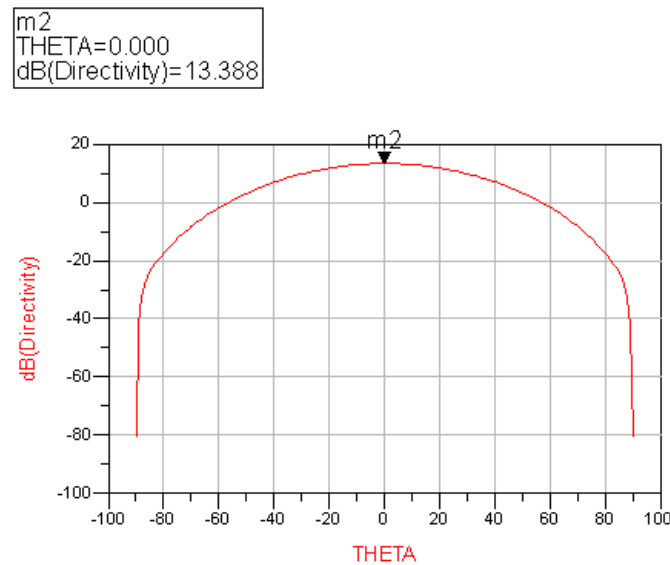


Figure 2-10: Directivity of a Single Element Patch Antenna

Patch antennas have low efficiency. The total efficiency of the antenna takes into account the losses at the input terminals and within the structure of the antenna. The losses may be due to the reflection because of the mismatch between the feeding transmission line and the antenna or it may be due to the Ohmic losses such as the conduction and dielectric losses [3]. The efficiency of the designed antenna is found out to be 64.9 % as shown in figure 2-11. The optimum range of efficiency for lw profile antennas is between 55 to 80 %. An efficiency of 65 % indicates that the antenna is optimally designed and most of the excitation energy is converted into electromagnetic Radiation.

```

m1
THETA=0.000
real(Efficiency)=64.917

```

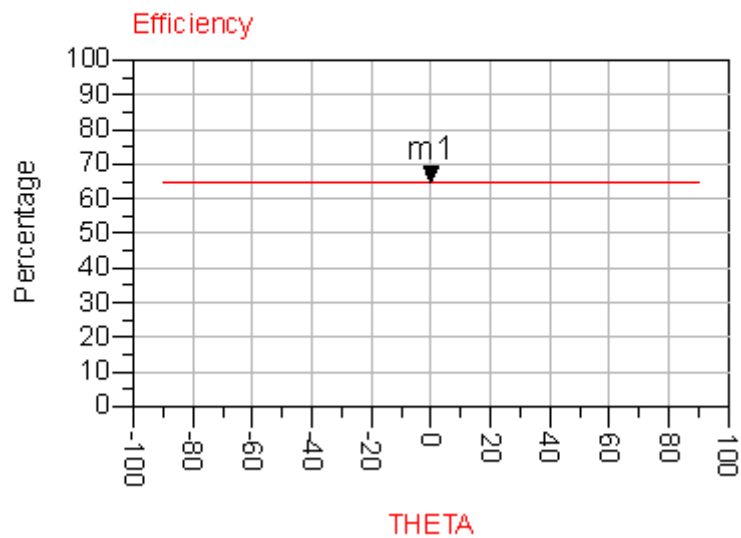


Figure 2-11: Efficiency of Patch Antenna

The power radiated by the antenna is 0.11 Watts per Steradian. Figure 2-12 shows the plot for the radiated power as well the radiation pattern of the single element patch antenna. As patch antenna is also known as a broadside radiator, its radiation pattern is normal to the surface of the antenna. The radiation pattern shows that the power is radiated almost equally throughout.

```

m1
THETA=0.000
real(Power)=0.110

```

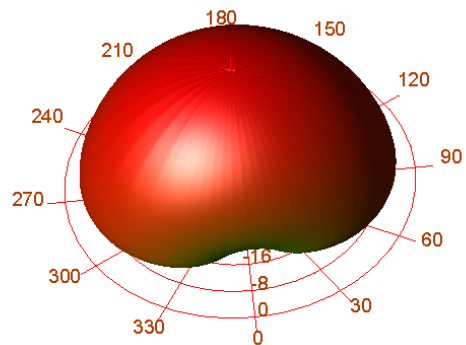
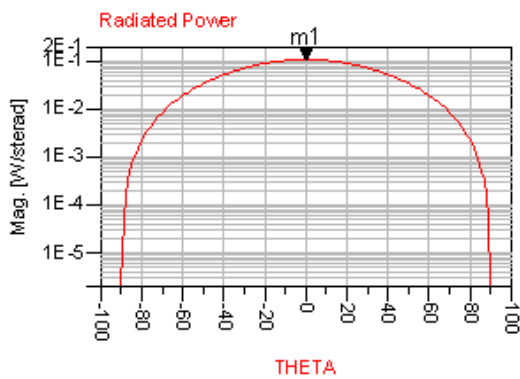


Figure 2-12: Power Radiated and Radiation Pattern

2.7. Antenna Array

Single element antennas have low gain and low directivity. Antenna arrays are designed to increase the gain and directivity. Arrays are versatile and are used to synthesize a required beam pattern that cannot be achieved with a single antenna element. There are two ways of feeding an array; a series feed network and a corporate feed network. The feed network designed in this project is the corporate feed network. Corporate feed networks are used to provide power splits of 2^n , where n is the number of antenna elements [3].

2.8. Design of Antenna Array in ADS

A four element antenna array is designed in Agilent ADS software. The separation between the antenna elements is kept 0.5λ to avoid coupling the different antenna elements. Figure 2-13 shows the coupling between the different antenna elements. The figure shows that the coupling between the adjacent antenna elements is maximum and the coupling between the farthest antenna elements is minimum.

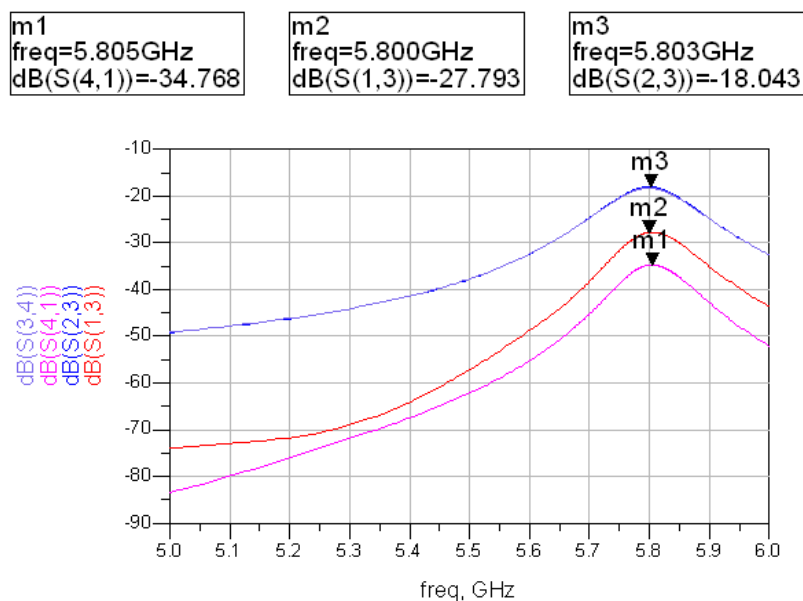


Figure 2-13: Coupling between Antenna Elements

The complete array is designed and simulated in ADS using a corporate feed network. Figure 2-14 shows the array design in ADS. The power from the array elements is combined using Wilkinson Power combiners. Corporate fed Wilkinson Combiners have been designed at a frequency of 5.8 GHz. The gain of the array is found out to be 13.2 dB which is 6 dB more than the gain of the single element patch antenna. When the number of antenna elements is doubled, there is a 3 dB increase in the gain as well as the directivity. So, when the number of antennas is increased from one to two, there is a 3 dB increase in the gain as well as directivity and when the number is increased to four, there is an increase of 6 dB in the gain as well as directivity. The gain of the array is shown in figure 2-15.

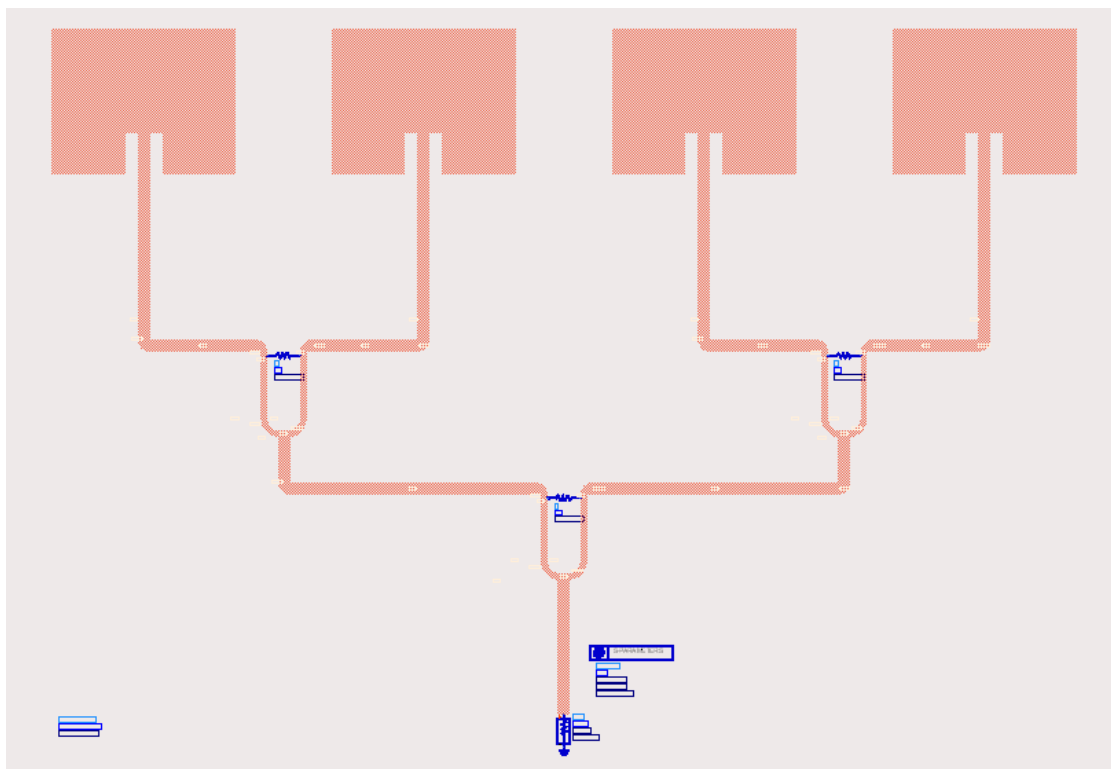


Figure 2-14: Complete Array Design

Figure 2-15 depicts the gain of the antenna array which employs four microstrip patch antennas. The gain is found out to be 13.2 db as mentioned above.

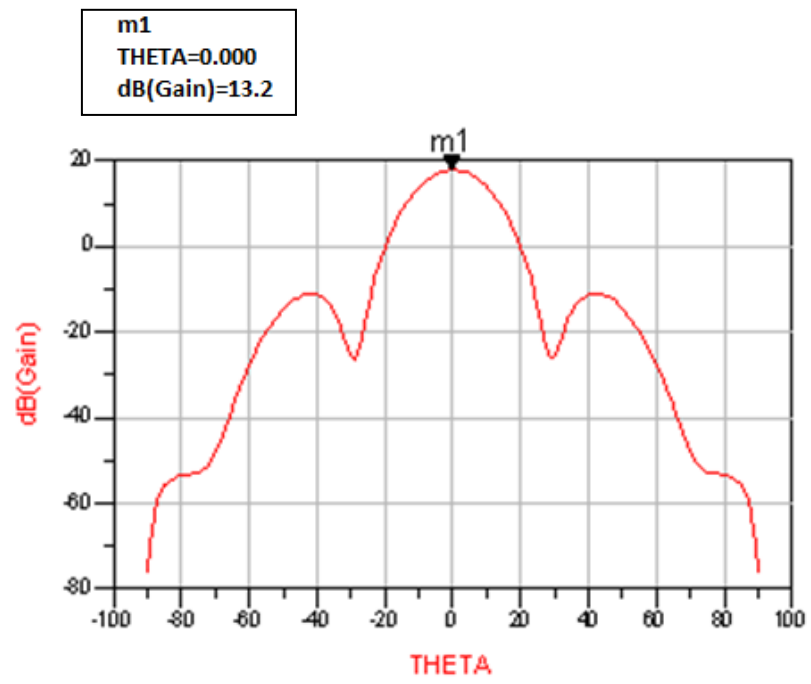


Figure 2-15: Gain of Array

PHASE SHIFTING SWITCH

A phase shifter is required to steer the beam at the required angle. In this project, PIN diodes are used as phase shifting devices. The model of the PIN diodes used is HPND 4028. PIN diode is one of the most prominent and efficient device in microwave switching. It has the lowest switching time. Using one PIN diode it is possible to switch the RF signal from zero level to a high level and vice versa in a very short span of time. In the project, each antenna element is followed by a phase shifting switch. Each phase shifting switch employs two PIN diodes. The biasing of the PIN diodes is controlled by the specially designed control circuitry which is discussed in chapter 8. This chapter focuses on the design of the Phase shifting switch and the simulated results in Agilent ADS software.

3.1. Always-Matched Switch

In this section, the comparison between a normal phase shifting switch and an Always-Matched phase shifting switch is presented. If a single PIN diode switch is used, the received power is wasted during the OFF state of the switch and the loss factor is nearly 10 dB. On the other hand, by using the Always-Matched switch instead of a simple switch, a 6-dB power increase at the output of switch is achieved and the loss factor is reduced to 4dB. In addition to this, the antenna and the power combiner ports are always matched using this switch. This switch also attenuates or totally removes some of the undesired replicas [7].

Figure 4-1 shows a switch design that fulfills the always matched condition. In the figure, diodes D1 and D2 are biased oppositely. Diode D2 is connected to ground through impedance Z_0 . When diode D1 is OFF, the other diode D2 connects the

impedance Z_0 to the power combiner terminal and vice versa. So, the power combiner terminals are always matched. While the switch circuit in 3-1 figure satisfies the always matched condition, it still exerts the aforesaid 10 dB loss on the desired replica.

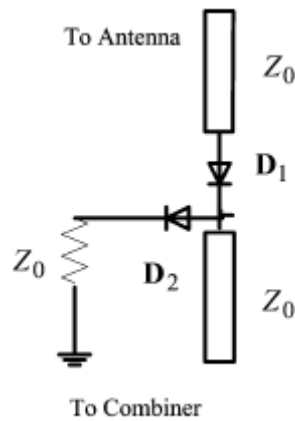


Figure 3-1: First Design for Always-Matched Switch

Now, figure 3-2 depicts another switch design that fulfills the always matched condition. In this circuit, both the PIN diodes are connected in parallel and they are biased oppositely and one diode is in series with a 180 phase shifting transmission line. When diode D1 is ON, it passes the RF signal but when diode D2 is ON, it passes the phase shifted RF signal. Therefore, this switch design has the loss factor of around 3.9 dB. For 180 phase shift a transmission line of length $\lambda_g/2$ is used [7]. Also, to hold always matched condition, when one diode is OFF, the equivalent impedance seen from the other end of the corresponding line is infinity or open circuit and so the impedance seen by the ON diode is always Z_0 .

Thus, the impedance mismatch condition is removed by using the above mentioned switch designs.

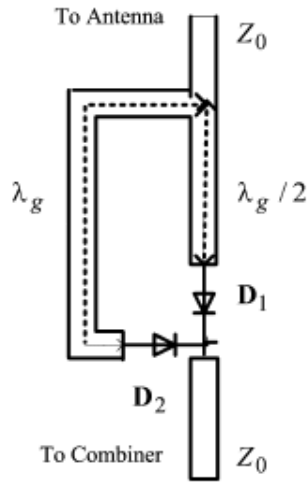


Figure 3-2: Second Design for Always-Matched Switch

3.2. Novel Phase Shifting Switch

In this design both the PIN diodes are controlled using one control signal. Therefore, the biasing of the two opposite PIN diodes is dependent. The length of the smaller arm is $\lambda_g / 2$ whereas the length of larger arm is λ_g . When negative pulse comes, the diode D_2 is ON and D_1 is OFF then RF signal is transferred to the output. When positive pulse comes, then D_1 is ON and D_2 is OFF, and as a result, 180° phase shifted signal is transferred to the output. Hence for 180° phase shift the $\lambda_g / 2$ arm is used. [7]

Figure 3-3 shows the design of the novel phase shifting switch. Two oppositely biased PIN diodes are employed in this design. The PIN diodes used are HPND 4028. HPND 4028 Beam Lead PIN diodes offer for low capacitance, low resistance and fast switching at microwave frequencies. These PIN diodes are operated at low bias levels for minimal power consumption and are simulated using S2P files provided by the manufacturer. The switching time of these PIN diodes is 2 nanoseconds. The capacitance is 0.025 pico Farads at 1 MHz. These PIN diodes offer a low resistance of 1.5 Ohms at a forward bias current of 10 mA.

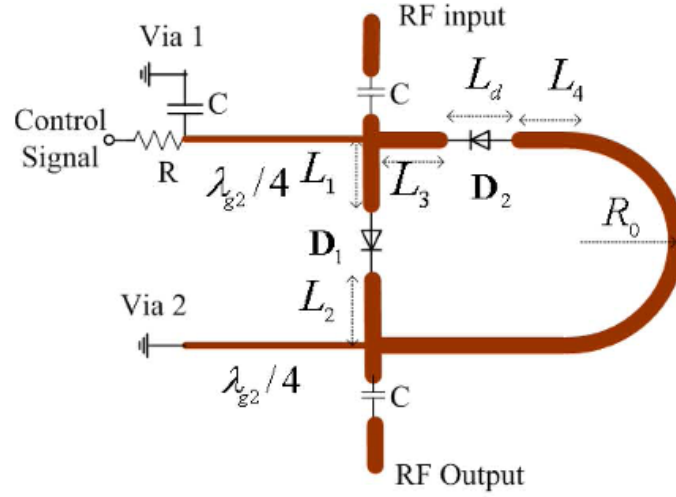


Figure 3-3: Novel Phase Shifting Switch

Pulse Train of adjustable delay and adjustable width is used to bias the PIN diodes and this pulse train is responsible for the alternative ON and OFF states of PIN diodes. The general form of the equivalent sampling pulse train on the n^{th} antenna element in one period can be written as

$$p_l(t) = \begin{cases} \alpha_1, & t_{sl} \leq t/T_s \leq t_{sl} + \tau_l \\ \alpha_2, & \text{otherwise} \end{cases} \quad (3.1)$$

Where T_s is the pulse train period, t_{sl} is the starting time or time delay of the pulse and τ is the duty cycle of pulse. Figure 3-4 shows the depiction of the pulse train.

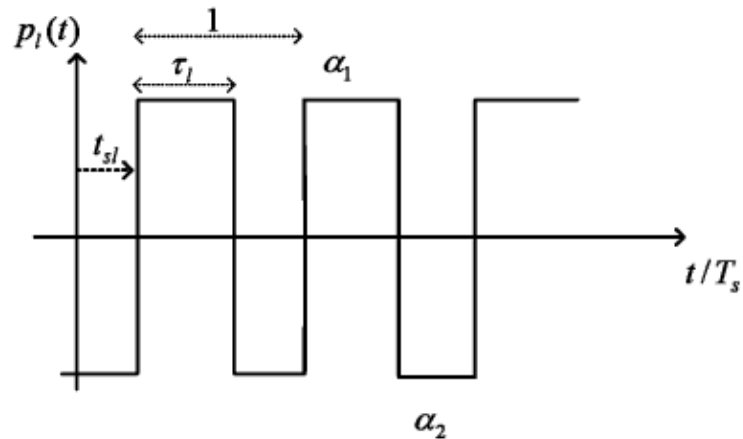


Figure 3-4: Pulse Train

3.3. Design of the Switch in ADS

The switch is optimized using the Agilent ADS software and then replicated for every antenna. Following are the dimensions of the phase shifting switch.

$$L_1 = 0.081 \lambda_g = 2.4777 \text{ mm}$$

$$L_2 = 0.083 \lambda_g = 2.4388 \text{ mm}$$

$$L_3 = 0.095 \lambda_g = 2.9059 \text{ mm}$$

$$L_4 = 0.077 \lambda_g = 2.3553 \text{ mm}$$

$$L_d = 14.4 \text{ mils}$$

$$W = 1.147 \text{ mm}$$

$$R = 0.5 (L_1 + L_2 + L_d + W) = 3.265 \text{ mm}$$

Figure 3-5 shows the design of the switch in ADS.

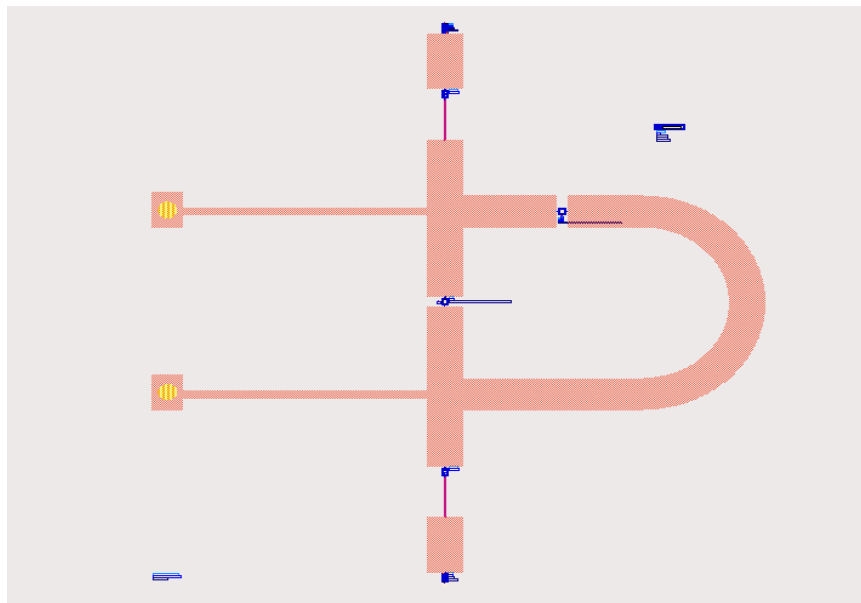


Figure 3-5: Switch Design in ADS

Working of the switch can be best explained by analyzing different states of the diodes D1 and D2. For each state, the insertion loss, return loss and output phase

results are shown in the following section.

3.3.1. First State

When diode D1 is ON and diode D2 is OFF. The results of this state are shown in figure 3-6. Insertion loss is -0.88 dB. Return Loss is less than -13 dB. The output phase of this state is 130.9 degrees.

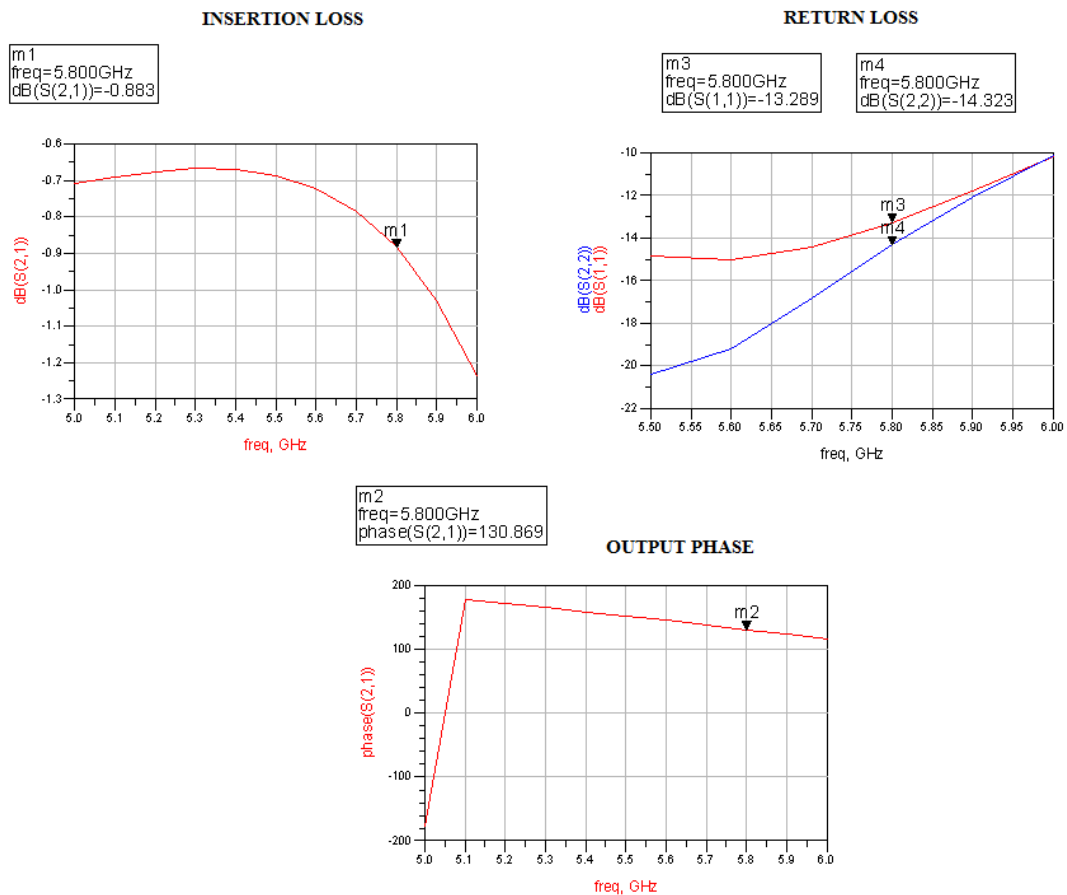


Figure 3-6: Results of State 1

3.3.2. Second State

When diode D1 is OFF and diode D2 is ON. The results of this state are shown in figure 3-7. Insertion loss is -1 dB. Return Loss is less than -12 dB. The output phase of this state is -51.1 degrees.

The overall phase shift is thus 180 degrees.

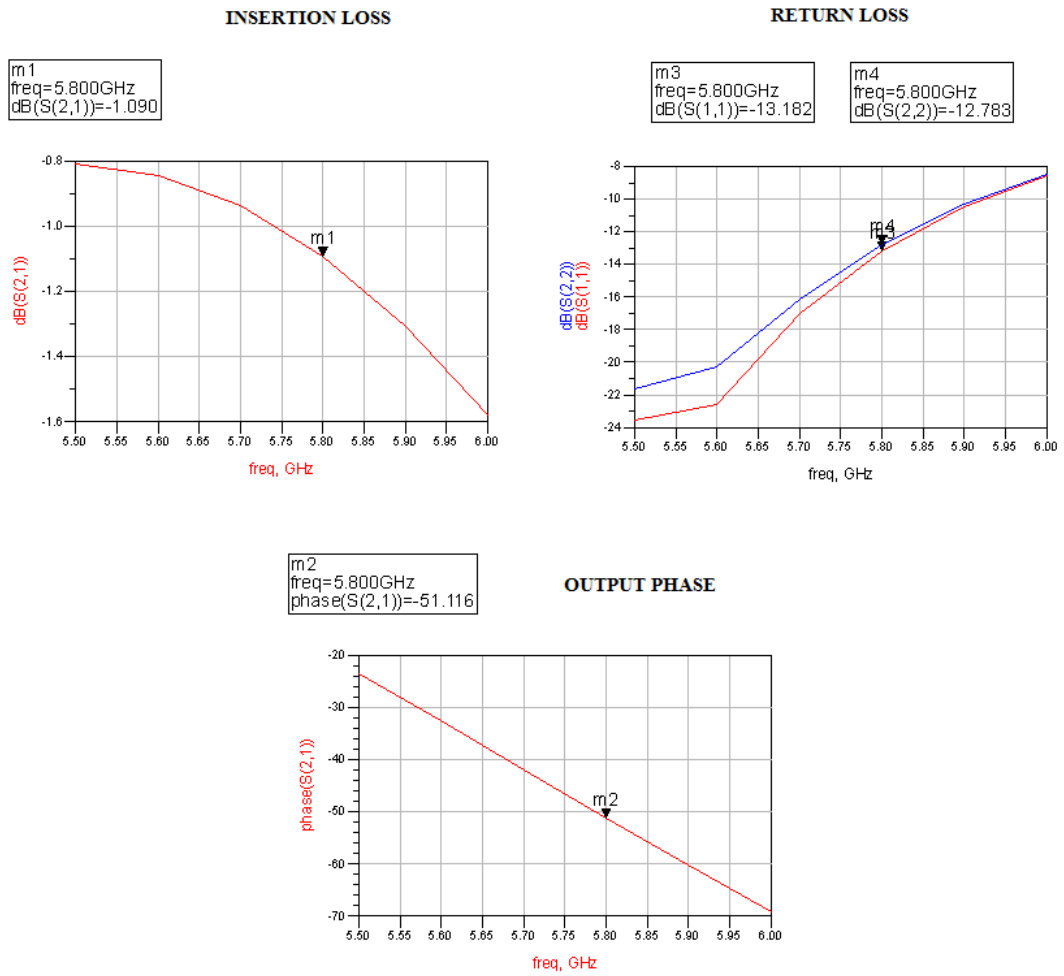


Figure 3-7: Results of State 2

WILKINSON POWER COMBINER

4.1. Power Dividers and Combiners

Power dividers and power combiners are passive microwave components used for power division or power combining. A 0° splitter is a passive device which accepts an input signal and delivers multiple output signals with specific phase and amplitude characteristics. The output signals theoretically possess the following characteristics: equal amplitude, 0° phase relationship between any two output signals, high isolation between each output signal, insertion loss

The insertion loss depends upon the number of output ports. Table 4-1 shows the relationship between the number of output ports and the insertion loss.

TABLE 4-1: Insertion Loss vs. Output Ports

Number of Output Ports	Theoretical Insertion Loss (dB)
2	3.0
3	4.8
4	6.0
5	7.0

Figure 4-1 shows a typical 3-port power divider. Port 1 is the input port and port 2 and port 3 are the output ports. The theoretical insertion loss of this 3 port network is 3 dB as given in table 4-1.

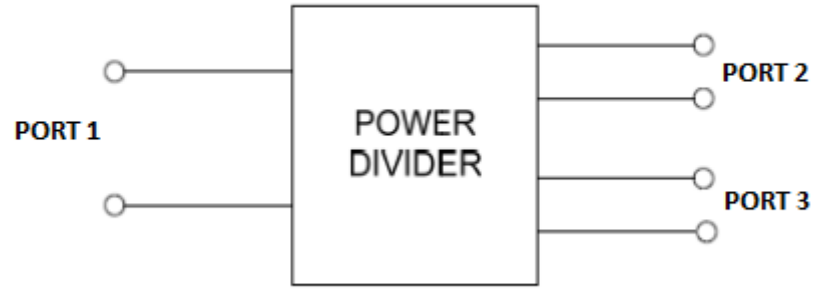


Figure 4-1: 3-Port Power Divider

Since the 0° power splitter is a reciprocal passive device it may be used as a power combiner simply by applying each signal singularly into each of the splitter output ports. The vector sum of the signals will appear as a single output at the splitter input port. Power dividers or splitters when used in reverse act as power combiners. Power dividers are often of equal division (3dB) type but unequal dividers are also used [6].

The S-parameter matrix of such a device is:

$$[S] = \begin{bmatrix} S_{11} & S_{12} & S_{13} \\ S_{21} & S_{22} & S_{23} \\ S_{31} & S_{32} & S_{33} \end{bmatrix} \quad (4.1)$$

We can easily show that a three port device which is reciprocal, matched and lossless is impossible to built [6]. Since all the three ports of this power divider are matched, $S_{ii} = 0$, and the network is nonreciprocal, $S_{ij} = S_{ji}$, the modified S-matrix can be written as:

$$[S] = \begin{bmatrix} 0 & S_{12} & S_{13} \\ S_{21} & 0 & S_{23} \\ S_{31} & S_{32} & 0 \end{bmatrix} \quad (4.2)$$

Also as the network is lossless then this matrix should be unitary and yields:

$$|S_{12}|^2 + |S_{13}|^2 = 1 \quad S_{13} S_{23}^* = 0 \quad (4.3)$$

$$|S_{12}|^2 + |S_{23}|^2 = 1 \qquad S_{13} S_{13}^* = 0 \qquad (4.4)$$

$$|S_{13}|^2 + |S_{23}|^2 = 1 \qquad S_{13} S_{23}^* = 0 \qquad (4.5)$$

Considering the above equations we see that the second column must have at least two out of three S parameters to be equal to zero. But if two of them were zero then one of the equations in the first column will be violated. Thus, we can conclude that it is impossible to satisfy all the three criteria of any power divider i.e. lossless, matched and reciprocal. Relaxing anyone of these constraints makes the other two achievable.

4.2. Types of Dividers

The following sections explain the different types of power dividers available for power division and power combining. These types are the T-junction, the lossless divider, resistive dividers, and Wilkinson power divider. These types are explained in the following sections.

4.2.1. Junction / T-line

The earliest transmission line power dividers were simple T-junctions. The T-junction power divider is a simple three-port network which can be used for power combining or power splitting. It can be implemented in microstrip (as shown in figure) as well as in other forms. According to the network theorem it is impossible to design a divider which is lossless, matched and isolated at the same time [7].

Figure 4-2 depicts a typical T-Junction.

The T-junction has sub-types which are the lossless divider, the resistive divider, the Wilkinson Power Divider. These sub-types are discussed in sections 4.2.2 through 4.2.4 along with the complete mathematical models.

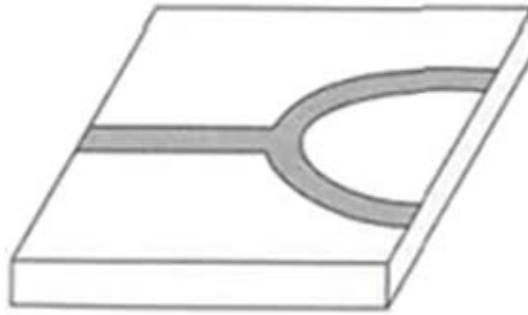


Figure 4-2: T-Junction

T-junction dividers are of the following types:

4.2.2. Lossless Dividers

The simplest type of power divider is the T junction. T junction can be implemented using virtually any type of transmission line. However, the T junction is very simple to implement, it must be treated with care because it does not offer any isolation between its ports. Figure 4-3 shows a lossless divider.

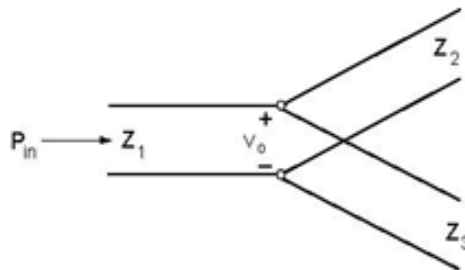


Figure 4-3: Lossless Divider

In order for the input port to be matched, the output lines must be matched (terminated in their characteristic impedance). The power dividing ratio can be selected by using different values of characteristic impedance for ports 2 and 3 [7].

$$P_1 = P_2 + P_3 = \alpha P_1 + \beta P_1 \quad (4.6)$$

$$\alpha + \beta = 1 \quad (4.7)$$

$$P_2 = \frac{1}{2} \frac{V_o^2}{Z_2} = \alpha P_1 = \alpha \frac{1}{2} \frac{V_o^2}{Z_1} \Rightarrow \alpha = \frac{Z_1}{Z_2} \quad (4.8)$$

$$P_3 = \frac{1}{2} \frac{V_o^2}{Z_3} = \beta P_1 = \beta \frac{1}{2} \frac{V_o^2}{Z_1} \Rightarrow \beta = \frac{Z_1}{Z_3} \quad (4.9)$$

For matching requirements:

$$\Gamma_1 = \frac{Z_L - Z_1}{Z_L + Z_1} = \frac{(Z_2 \parallel Z_3) - Z_1}{(Z_2 \parallel Z_3) + Z_1} = \frac{Z_2 Z_3 - Z_1 Z_2 - Z_1 Z_3}{Z_2 Z_3 + Z_1 Z_2 + Z_1 Z_3} = 0 \quad (4.10)$$

$$Z_2 Z_3 = Z_1 (Z_2 + Z_3) \Rightarrow Z_1 = \frac{Z_2 Z_3}{Z_2 + Z_3} \quad (4.11)$$

For the matching of port 2:

$$\Gamma_2 = \frac{Z_L - Z_2}{Z_L + Z_2} = \frac{(Z_1 \parallel Z_3) - Z_2}{(Z_1 \parallel Z_3) + Z_2} = \frac{Z_2 Z_3 - Z_1 Z_2 - Z_2 Z_3}{Z_2 Z_3 + Z_1 Z_2 + Z_2 Z_3} \quad (4.12)$$

Figure 4-4 shows the matching of lossless divider.

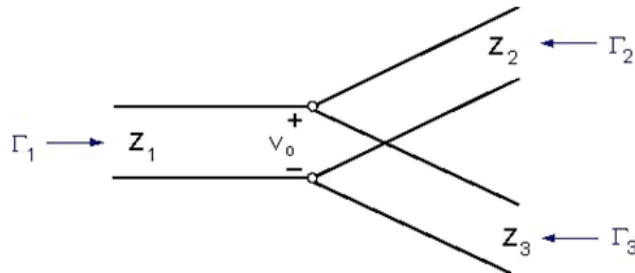


Figure 4-4: Matching of Lossless Divider

If port 2 is matched, then $\Gamma_2 = 0$ and we will have:

$$Z_1 Z_3 - Z_2 (Z_1 + Z_3) = 0 \quad \Rightarrow \quad Z_2 = \frac{Z_1 Z_3}{Z_1 + Z_3} \quad (4.13)$$

Substitution of $Z_1 = \frac{Z_2 Z_3}{Z_2 + Z_3}$ yields $Z_2 = 0$.

This shows that the lossless T-junction cannot be matched at all three ports simultaneously.

4.2.3. Resistive Dividers

As the name suggests resistive divider uses resistances. Resistive divider can be matched at all ports but on the expense of loss which makes it useless for power sensitive applications. Two configurations of resistive dividers are given in figure 4-5.

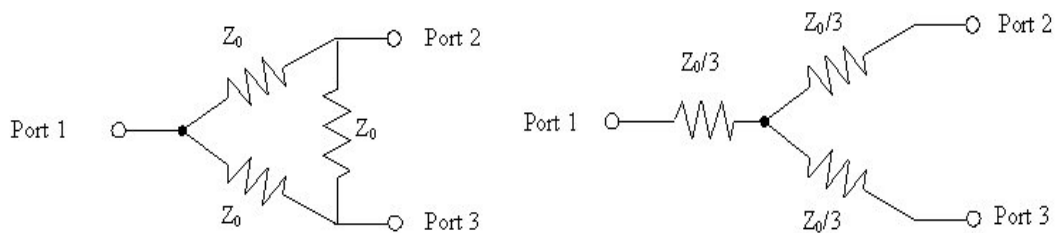


Figure 4-5: “Delta” and “Wye” Configurations of Resistive Divider

4.2.4. Wilkinson Power Divider

The Wilkinson power splitter was invented around 1960 by Ernest Wilkinson. It is a specific class of power divider circuit that can achieve isolation between the output ports while maintaining a matched condition on all ports. The Wilkinson design can also be used as a power combiner because it is made up of passive components and hence reciprocal [5]. Wilkinson relied on quarter wave transformers to match the split ports to a common port. Since a lossless reciprocal three port network cannot have all ports simultaneously matched, Wilkinson introduced a resistor for the purpose of matching. Apart from matching, the resistor also improved the isolation between the

output ports. Figure below shows the equivalent circuit and the microstrip implementation of a Wilkinson two-way power divider. The impedances required for the quarter wave transformer and the isolating resistor are also shown in figure 4-6.

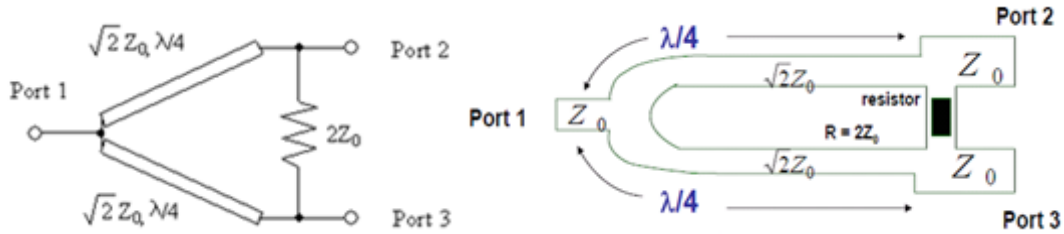


Figure 4-6: Three-Port Wilkinson Power Divider

The scattering parameters for the common case of a 2-way equal-split Wilkinson power divider at the design frequency are given by:

$$[S] = \frac{-j}{\sqrt{2}} \begin{bmatrix} 0 & 1 & 1 \\ 1 & 0 & 0 \\ 1 & 0 & 0 \end{bmatrix} \quad (4.14)$$

Inspection of the S matrix reveals that the network is reciprocal ($S_{ij} = S_{ji}$), that the terminals are matched ($S_{11}, S_{22}, S_{33} = 0$), that the output terminals are isolated ($S_{23}, S_{32} = 0$), and that equal power division is achieved ($S_{21} = S_{31}$). The non-unitary matrix results from the fact that the network is lossy. No loss occurs when the signals at ports 2 and 3 are in phase and share equal magnitude.

An ideal Wilkinson divider would yield:

$$S_{21} = S_{31} = -3dB = 10 \log_{10} \left(\frac{1}{2} \right) \quad (4.15)$$

The two arms are quarter-wave transformers of impedance $1.414Z_0$ with length $\lambda/4$. When a signal enters port 1, it splits into equal-amplitude, equal-phase output signals at ports 2 and 3 [7]. Since each end of the isolation resistor between ports 2 and 3 is at

the same potential, no current flows through it and therefore the resistor is decoupled from the input. The two output port terminations will add in parallel at the input, so they must be transformed to $2Z_0$ each at the input port to combine to Z_0 . The quarter-wave transformers in each leg accomplish this. Without the quarter-wave transformers, the combined impedance of the two outputs at port 1 would be $Z_0/2$. The characteristic impedance of the quarter-wave lines must be equal to $1.414Z_0$ so that the input is matched when ports 2 and 3 are terminated in Z_0 .

The Table 4-2 summarizes the characteristics of different types of power dividers and combiners.

Table 4-2: Summary of Dividers

<u>POWER DIVIDER</u>	<u>LOSS</u>	<u>MATCHING</u>	<u>ISOLATION</u>
Lossless Divider	Lossless	Not Matched	No Isolation
Resistive Divider	Lossy	Matched	No Isolation
Wilkinson Power Divider	Lossless (virtually)	Matched	Isolated

POWER COMBINER AND FEED NETWORK DESIGN

5.1. Design of Wilkinson Power Combiner in ADS

Wilkinson power dividers are designed in ADS using microstrip lines. Z_0 is taken to be 50Ω (standard) and the impedance of the two arms was calculated by using the formula $1.414Z_0$. The background and the detailed working of the combiner has been discussed in the previous chapter. Resistor in the center of each combiner is of the value of twice Z_0 which is equal to 100Ω . The design parameters for the Wilkinson Power combiner are shown in Table 5-1.

Table 5-1: Design parameters for Wilkinson Power Divider

<u>IMPEDANCE</u>	<u>MAGNITUDE</u>	<u>WIDTH IN mm</u>
Z_1	50Ω	1.62
Z_2	70.7Ω	0.832

The figure 5-1 shows the layout of the combiner in ADS.

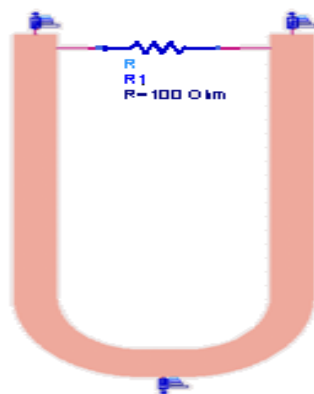


Figure 5-1: Wilkinson Power Combiner Layout in ADS

The design is optimized at 5.8GHz and good results are achieved. Insertion loss calculated is around -3dB. Insertion loss is shown in figure 5-2.

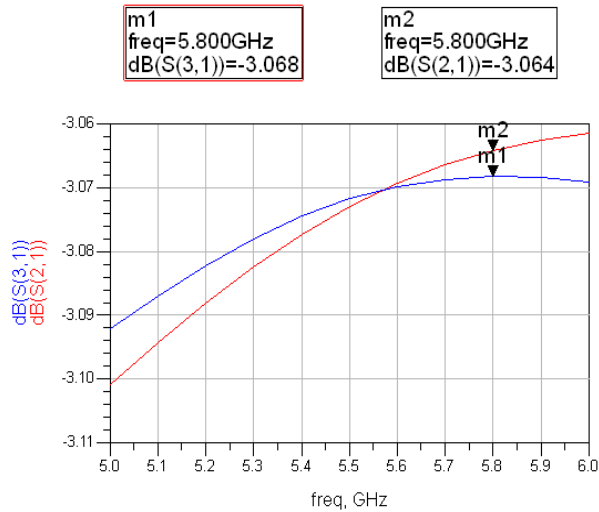


Figure 5-2: Insertion Loss of WPC

Return loss of each divider in ADS is about -30dB as shown in the figure 5-3. The low return loss shows the reflections at the input of the power combiner are minimum and most of the input power is transferred to the output.

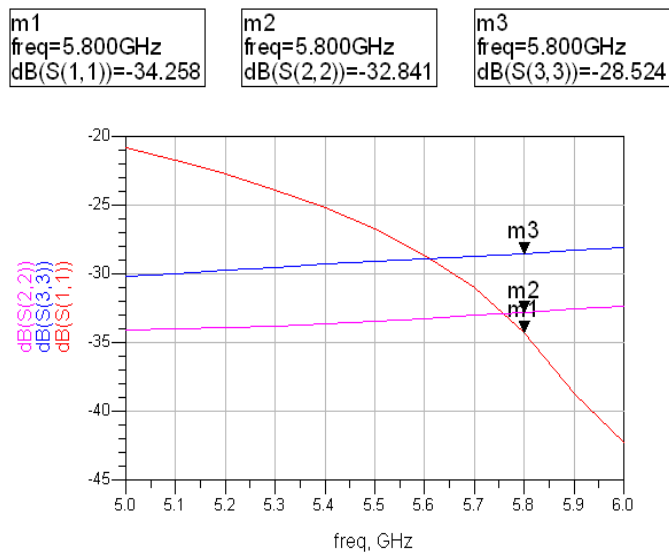


Figure 5-3: Return Loss of WPC

Port to port isolation or S_{23} is -41 dB. Figure 5-4 shows the graph for port to port isolation. The small value of the port to port isolation shows that the leakage of power from one output port to the other is minimal.

```

m1
freq=5.800GHz
dB(S(2,3))=-40.974

```

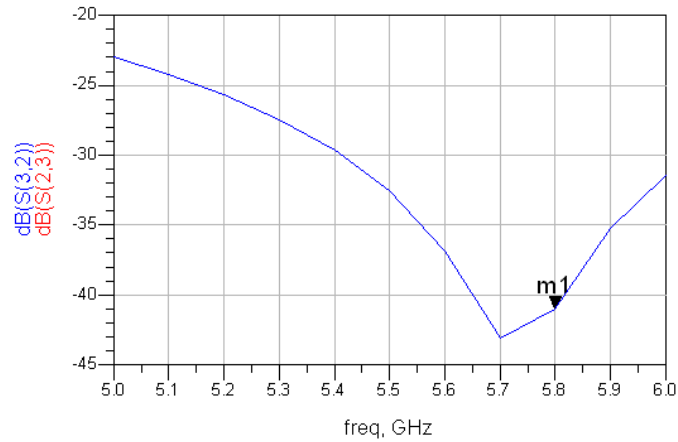


Figure 5-4: Port to Port Isolation

5.2. Feed Network Design

An antenna array feed network is often used to regulate the amplitude and phase feed requirements of the radiating elements (patches). Thus selecting, optimizing and implementing the feed network forms a critical part of the antenna array design. Amongst the most common and well-known feeding techniques, the corporate feeding is widely used in scanning phased, multi-beam or shaped-beam arrays. In this study, corporate feed network is used to construct a beam scanning linear phase array antenna. The feed network is designed to combine the Wilkinson power divider with PIN diode based phase shifters. The layout of the feed network is shown in Figure. The antenna array signals are combined using a corporate feed, which is composed of three two-way Wilkinson combiners. The four patch antennas are paired and are combined using a Wilkinson Power Combiner. The output of these two combiners is further combined with a third Wilkinson Power Combiner to give a single path for the signal. The length of the lines connecting the Wilkinson power dividers were optimized for maximum return loss at the input and equal power division at the four output ports. Figure 5-5 shows the layout of the Wilkinson power combiner in ADS.

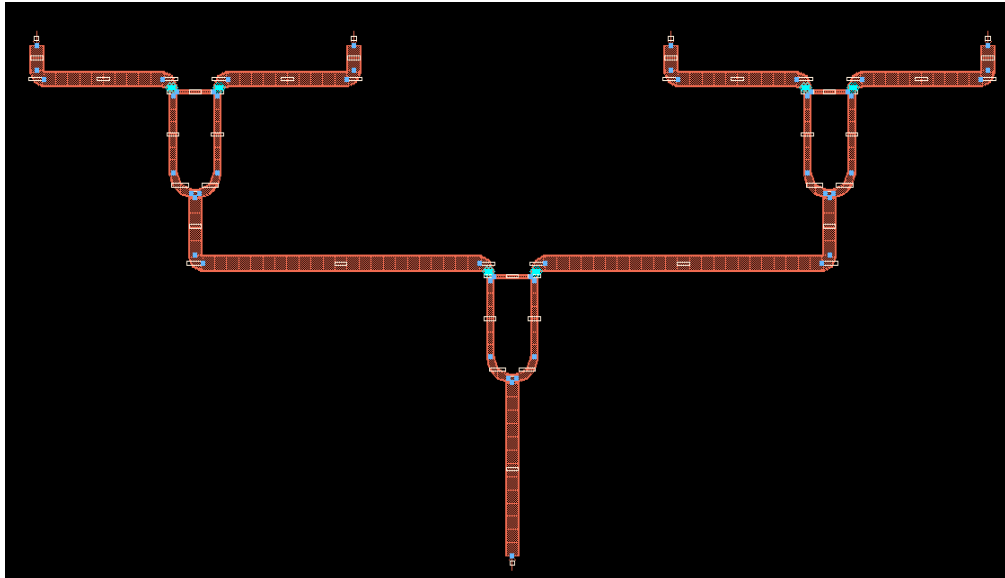


Figure 5-5: Layout of Complete Feed Network in ADS

The return loss of the complete feed network has been observed to be -37.6 dB at 5.8GHz frequency. A low return loss shows that the Wilkinson Power Combiner is optimized at the operating frequency of 5.8 GHz. Figure 5-6 shows the S_{11} parameter of the feed network:

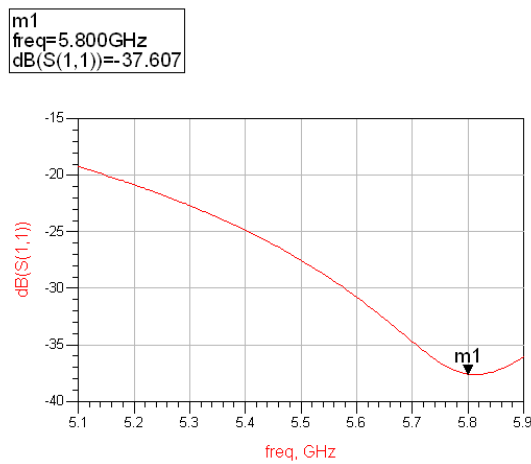


Figure 5-6: Return Loss of Complete Feed Network

MICROWAVE DOWN-CONVERTER

6.1. Overview

After the RF signal is received, it has to be amplified using a low noise amplifier because the signal gets deteriorated due to losses like free space loss, atmospheric absorption losses and connector or cable losses. The signal is then down-converted from RF frequencies and brought to an Intermediate frequency, simply known as IF. The IF signal is again amplified using an IF amplifier and then the signal is fed to a Low pass filter to recover the baseband signal.

In this project, the received RF signal of 5.8 GHz is first amplified using an LNA. Then a double balanced mixer is used to down-convert the signal to 60 MHz and the output of 60MHz is again amplified with the help of IF amplifier. Finally the baseband is recovered through a low pass filter.

The block diagram of the complete down-converter is shown in figure 6-1. The different blocks show the different components used in the downconverter.

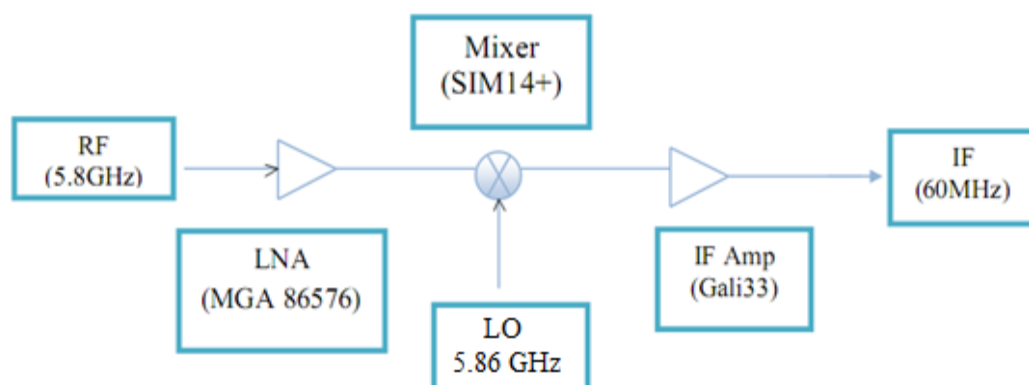


Figure 6-1: Block Diagram of Down-Converter Part

6.2. Low Noise Amplifier

The first stage after the receiver is the LNA. It's possible that some type of filter or receiver protection device is between the LNA and the antenna but it is rarely attempted. The signal received is very weak and requires to be amplified with minimum noise addition [8].

The characteristic features of the LNA are Noise figure, Gain, Linearity (measured in P1dB), Bandwidth, Flat gain, VSWR.

6.2.1. Noise Figure and Gain

The noise factor is a measure of how the the signal to noise ratio is degraded by a device:

$$\text{Noise factor} = \frac{S_{in} / N_{in}}{S_{out} / N_{out}} \quad (6.1)$$

Where

S_{in} is the signal level at the input

N_{in} is the noise level at the input,

S_{out} is the signal level at the output

And N_{out} is the noise level at the output.

The noise factor of a device is specified with noise from a noise source at room temperature ($N_{in}=KT$), where K is Boltzmann's constant and T is approximately room temperature in Kelvin.

Signal to noise ratio always worsens from input to output due to entropy; as the S/N ratio at output is less than S/N ratio at input, so noise factor is always greater than unity [9].

Noise figure is the noise factor, expressed in decibels:

$$\text{NF (decibels)} = \text{Noise Figure} = 10 \cdot \log (\text{noise factor}) \quad (6.2)$$

If the antenna system or receiver has an RF amplifier in it, electrons passing through the device create random noise, some of which falls within the frequency we wish to receive. More intense this internally generated noise, more strength of the received signal is needed to overcome this "noise figure". Increasing the gain will not improve the received signal if the noise figure of the circuit is high.

A cheap compromise to lower the noise figure in an RF amplifier is to lower the current going through it. Unfortunately, this leaves us with an amplifier that has very low power output, and poor IP3, which are the basic factors that cause a device to mix signals together and cause inter-modulation. The result is a system that invites even moderate signals to overload and degrade the entire system. [9]

The designed receiver uses a mixer stage to convert the higher frequencies to a much lower Intermediate Frequency or "IF". This "Superheterodyne" conversion process results in a typical 6 to 8 db signal loss when diode mixers are used. Therefore it is desirable to amplify the signal ahead of this type of mixer, to make up for this loss.

Limiting the signals entering the amplifier and mixer stages to those frequencies which we wish to receive greatly reduces spectrum noise from other transmitters and RF noise sources. This increases the sensitivity for the desired frequency.

6.2.2. Linearity

Linearity of any amplifier is measured in terms of P1dB [9]. P1dB (Output Power at 1dB compression) is typically used when referring to LNAs. It is simply defined as the output power level at which the actual gain achieved deviates from the small signal gain by 1dB.

All active components have a linear dynamic range. This is the range over which the output power varies linearly with respect to the input power. As the output power increases to near its maximum capability, the device begins to saturate.

The point where the saturation effects are 1 dB from linear response is defined as the 1 dB compression point. From this point onwards, because of the nonlinear relation between the input and output power, the following relationship holds:

$$P_{\text{out 1 dB}} = P_{\text{in 1 dB}} + \text{Linear Gain} - 1 \text{ dB} \quad (6.3)$$

6.2.3. Bandwidth and Flat Gain:

The bandwidth of LNA is an important parameter which is also taken into account when choosing an LNA block or IC for a receiver. The bandwidth should be in accordance with the type of application the design is meant for. For wideband LNAs the gain should be flat otherwise problems may arise. Flat gain is therefore also taken into account when choosing LNA [10].

6.2.4. Voltage Standing Wave Ratio:

VSWR is used as an efficiency measure. Any RF component if mismatched tends to reflect radio waves back toward the source end of the cable, preventing all the power

from reaching the destination end. VSWR measures the relative size of these reflections. Ideal case would have a VSWR of 1:1. A good LNA has VSWR less than 1.5 [10].

6.2.5. MGA-86576 LNA IC

The LNA used in the design is MGA-86576. It is an economical, easy-to-use GaAs MMIC amplifier that offers low noise and excellent gain for applications from 1.5 to 8 GHz.

The MGA-86576 can be used without impedance matching as a high performance 2dB NF gain block. Alternatively, with the addition of a simple series inductor at the input, the device noise figure can be reduced to 1.6 dB at 4 GHz. A patented, on-chip active bias circuit allows operation from a single +5V power supply. Current consumption is only 16 mA.

The features of the MGA-86576 are as follows:

1.6 dB Noise Figure at 4GHz

23 dB Gain at 4GHz

+6 dBm P1dB at 4 GHz

Single +5 V Bias Supply

6.3. Frequency Mixer

A frequency mixer is a 3-port electronic circuit—two of the ports are “input” ports and the other port is an “output” port 1. The ideal mixer “mixes” the two input signals such that the output signal frequency is either the sum (or difference) of the two input frequencies [10]. In other words:

$$f_{\text{out}} = f_{\text{in1}} \pm f_{\text{in2}} \quad (6.4)$$

The nomenclature for the 3 mixer ports are the Local Oscillator (LO) port, Radio Frequency (RF) port and the Intermediate Frequency (IF) port.

The LO port is typically driven with either a sinusoidal continuous wave (CW) signal or a square wave signal. The choice to apply a CW or square wave signal depends on the application and the type of mixer. Conceptually, the LO signal acts as the “gate” of the mixer in the sense that the mixer can be considered “ON” when the LO is a large voltage and “OFF” when the LO is a small voltage. The LO port is exclusively used as an input port. Microwave mixers translate the frequency of electromagnetic signals [10].

The other 2 ports of the mixer, the RF and IF, can be interchanged as either the second input or the output. The actual configuration depends on the application. When the desired output frequency is lower than the second input frequency, then the process is called down-conversion and the RF is the input and the IF is the output. The relationship between input and output frequencies is given by:

$$f_{\text{IF}} = |f_{\text{LO}} - f_{\text{RF}}| \quad (6.5)$$

On the other hand, when the desired output frequency is higher than the second input frequency, then the process is called up-conversion and the IF is the input and the RF is output. During frequency down-conversion, the information carried by the RF signal is frequency translated to the IF output. Therefore, mixers perform the critical function of translating the frequency. The Intermediate Frequency lies in the range of Mega Hertz (MHz). Generally, the Intermediate Frequency is kept to be 60 MHz or 30 MHz. The IF is then fed to a Low Pass Filter (LPF) to recover the baseband.

6.3.1. Mixer Properties

This section explains the different properties of frequency mixers which are the Conversion Gain, 1 dB compression, Spurious Products, Isolation and Noise Figure.

6.3.1.1. Conversion Gain

Conversion gain of the RF Mixer is dependent on the type of the mixer (active or passive), and is also dependent on the load of the input RF circuit as well the output impedance at the RF port. It also depends on the level of the LO. The typical conversion gain of an active Mixer is approximately +10dB when the conversion loss of a typical diode mixer is approximately -6dB [13]. The Conversion Gain or Loss of the RF Mixer measured in dB is given by:

$$\text{Conversion gain [dB]} = \text{Output IF power delivered to the load [dBm]} - \text{Available RF input signal power [dBm]} \quad (6.6)$$

6.3.1.2. 1 dB Compression

Under normal (linear) operation, the conversion loss of the mixer will be constant, regardless of input RF power. If the input RF power increases by 1 dB, then the output IF power will also increase by 1 dB (and the power difference is the conversion loss). However, as the RF power becomes too large, this relationship does not hold. The 1 dB compression point is a measure of the linearity of the mixer and is defined as the input RF power required to increase the conversion loss by an extra 1 dB from ideal. Mixer compression is most easily represented graphically as shown in Figure below. For low input RF power, the slope of the line is 1:1. However, as the RF power increases, the mixer deviates from this linear behavior and the conversion loss starts to increase. When the input / output curve

sags by 1 dB (i.e. the conversion loss increases by 1 dB), the input RF 1 dB compression is reached [10]. Figure 6-2 shows mixer compression.

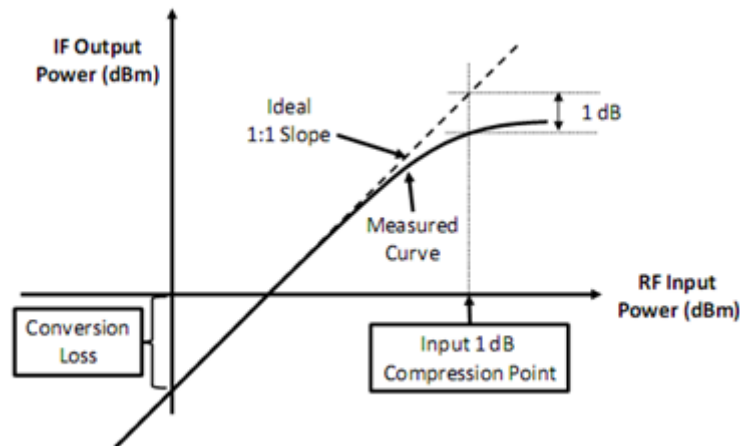


Figure 6-2: Mixer Compression

Conceptually, the 1 dB compression point occurs when the RF signal can no longer be considered as “small signal”. Under linear operation, the LO power is so much stronger than the RF power that the diode switching action is totally dominated by the LO. However, in compression, the RF power is commensurate with the LO power such that the diode switching action is compromised [10]. When the RF power is too high, the mixer balance degrades and the mixer circuit behaves like a single diode mixer. Among other things, operating the mixer in compression causes increased levels of intermodulation distortion, higher conversion loss, and degraded isolation performance. This behavior is explained by the fact that the compressed mixer spreads energy in the frequency domain because the diodes are being partially turned on by the RF signal.

6.3.1.3. Spurious Products

Spurious products in a Mixer are problematic, and mixer vendors frequently provide tables showing the relative amplitudes of each response under given LO drive

conditions. One way to reduce such products is to short-circuit the higher harmonics of the LO at the intrinsic mixer terminals to lower the power in such responses. Reducing the second or third harmonic of the local oscillator reduces its harmonic products by 20 to 25 dB and 10 to 15 dB, respectively [12].

6.3.1.4. Isolation

Isolation is a measure of the amount of power that leaks from one mixer port to another. There are multiple types of isolation: LO-to-RF, LO-to-IF, RF-to-IF.

Port isolation is obtained through mixer balance and the use of hybrid junctions. There will always be some small amount of power leakage between the RF, LO and IF ports. Isolation is the difference in power between the input signal and the leaked power to the other ports. Isolation is approximately reciprocal: the port 1 to port 2 isolation will track closely with the port 2 to port 1 isolation. Hence, a single measurement can be performed to determine the isolation in both directions [10].

6.3.1.5. Noise Figure

Noise figure is a measure of the noise added by the mixer itself. For a passive mixer which has no gain and only loss, the noise Figure is almost equal to the loss. In a mixer noise is replicated and translated by each harmonic of the LO that is referred to as Noise Folding [12].

In addition to the degradation in system noise Figure due to the conversion loss of the mixer, noise sources within the mixer device itself further corrupt the noise Figure. A mixer will convert energy in the upper or lower sidebands with equal efficiency. Consequently the noise in the side band with no signal will be added to the IF output, which will increase the Noise Figure at the IF port by 3dB, no matter how good the

preceding component noise figure is. An Image Filter at the RF input of the Mixer suppresses this noise.

6.3.2. Types of Mixers

This section explains the different types of frequency mixers based on their construction and working.

6.3.2.1. Single-Device (Diode) Mixer

The simplest mixer consists of a single diode as shown in figure 6-3.

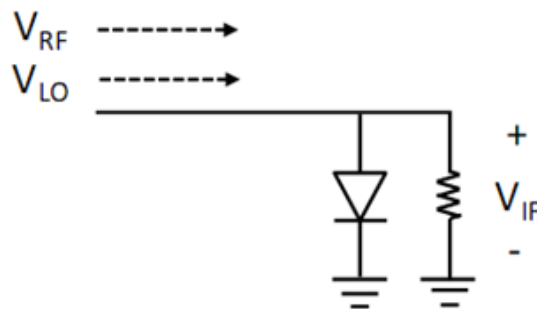


Figure 6-3: Equivalent Circuit of a Single Diode Mixer

A large signal LO and a small signal RF combine at the anode of the diode. For an “ideal” single diode mixer, it is assumed that the LO is significantly stronger than the RF such that only the LO has the ability to affect the trans-conductance of the diode [12]. The lower the RF power, the better the spurious performance (since the LO will control the diode transconductance more effectively).

6.3.2.2. Balanced Mixers

High performance mixers are designed using four and sometimes eight diodes. Sophisticated mixer designs make use of circuit symmetry to create “balance”. In fact,

virtually all commercially available mixers make use of some kind of mixer balancing. Mixer balancing offers several advantages such as: Inherent isolation between all mixer ports (and hence band flexibility), cancellation of most intermodulation products, common mode signal rejection, improved conversion efficiency, rejection of spurious responses and intermodulation products, better LO-to-RF, RF-to-IF and LO-to-IF isolation, rejection of AM noise in the LO.

The disadvantage of balanced mixers is their greater LO power requirements. In mixers, extra circuitry is needed to route and separate input and output signals from the diodes. In single diode mixers, this extra circuitry typically comes in the form of some kind of passive coupling, power division and/or filtering. It is difficult to create wideband single diode mixers with independent RF, LO and IF bands because the multiplexing circuitry is frequency specific. Moreover, such circuitry causes extra losses that reduce mixer efficiency. Balanced mixers are divided into two classes, called Single-Balanced mixers (SBM) and Double-Balanced Mixers (DBM).

Single Balanced Mixers are wideband mixers with low loss and independent input and output frequency bands are created using the classic four port hybrid junction [12]. The hybrid junction (also called the “magic tee”) is a four port circuit that provides mutual isolation between input ports and equal power division at the output ports. The input LO and RF sources will be isolated from one another, thus providing frequency band independence and equal power division to the load. Figure 6-4 shows a 4 port hybrid junction.

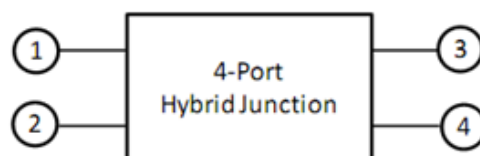


Figure 6-4: 4-Port Hybrid Junction

The Table 6-1 shows the input / output transfer characteristics of a 4-port hybrid junction.

Table 6-1: The Input / Output Transfer Characteristics of a 4-Port Hybrid Junction.

Port 1	Port 2	Port 3	Port 4
Input	Isolated	Input / 2	Input / 2
Isolated	Input	Input / 2	-Input / 2

The output signals are differentially phased (i.e. 180° phase shifted) when a signal is input to port 2. Output signals are in phase for inputs into port 1. The hybrid junction provides a natural method by which to create the single balanced mixer. This is shown in figure 6-5.

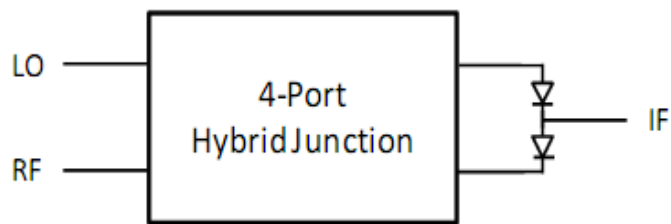


Figure 6-5: Mixer Constructed from a 4-Port Hybrid Junction

In this case, two diodes are used instead of one.

Double Balanced Mixers are formed from the combination of two Single Balanced Mixers as shown in figure 6-6.

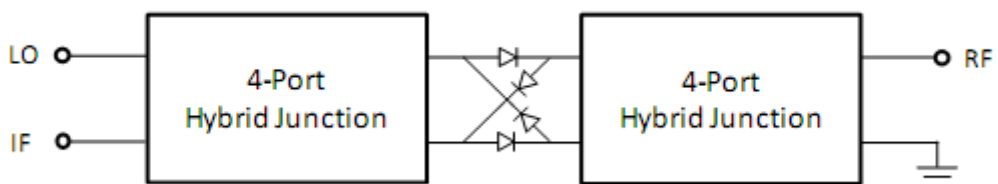


Figure 6-6: Construction of a Double Balanced Mixer from 4-Port Hybrid Junction

In this case, hybrid junctions are placed on both the RF and LO differential ports and the IF is obtained at the in phase port of the hybrid junction. Double balancing the mixer has the benefit of reducing nearly 75% of the spurious interferers possible at the IF port. Owing to the conservation of energy, double balanced mixers have better conversion efficiency than single ended or single balanced mixers [14].

6.3.3. SIM 14+ Mixer IC

The mixer IC used in this project is the SIM 14+ mixer. SIM-14+ is a low cost surface mount ceramic wideband double balanced frequency mixer having the following features: Wide bandwidth, 3700 to 10000 MHz, low conversion loss, typically 6.7 dB, high LO-RF isolation, typically 38 dB, excellent IF bandwidth, DC to 4000 MHz.

The Table 6-2 shows the typical electrical specifications of the SIM 14+ Mixer IC.

Table 6-2: Electrical Specifications of the SIM 14+ Mixer IC

Frequency (MHz)	Conversion Loss (dB)	LO-RF Isolation (dB)	LO-IF Isolation (dB)	IP3 at center Band (dBm)
3700-6200	6.7	38	16	16

The figure 6-7 shows the equivalent electrical schematics of the SIM 14+ Mixer IC.

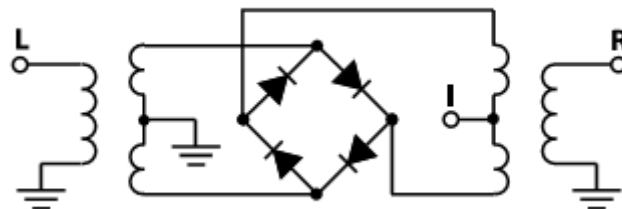


Figure 6-7: Electrical Schematics of SIM 14+

The LO to the mixer IC is 5.86 GHz and the IF is achieved at 60 MHz. This IF is then further amplified through IF amplifier.

6.4. IF – Amplifier

Conversion to an intermediate frequency is useful for many reasons. When several stages of filters are used, they can all be set to a fixed frequency, which makes them easier to build and to tune [12]. It's easier to make sharply selective filters at lower fixed frequencies. Converting to a lower intermediate frequency offers an advantage where the available amplifier devices have upper frequency gain limits comparable to the frequency in use. A lower IF can offer higher gain per stage than is possible at the RF stage [13]. The IF amplifier used in the design is GALI-33. It is a broadband DC to 4 GHz amplifier with up to 18.2 dBm typical output power [13].

6.5. Design of the Downconverter

The complete Downconverter has been designed and simulated in Agilent ADS. The figure 6-8 shows the schematics of the complete downconverter.

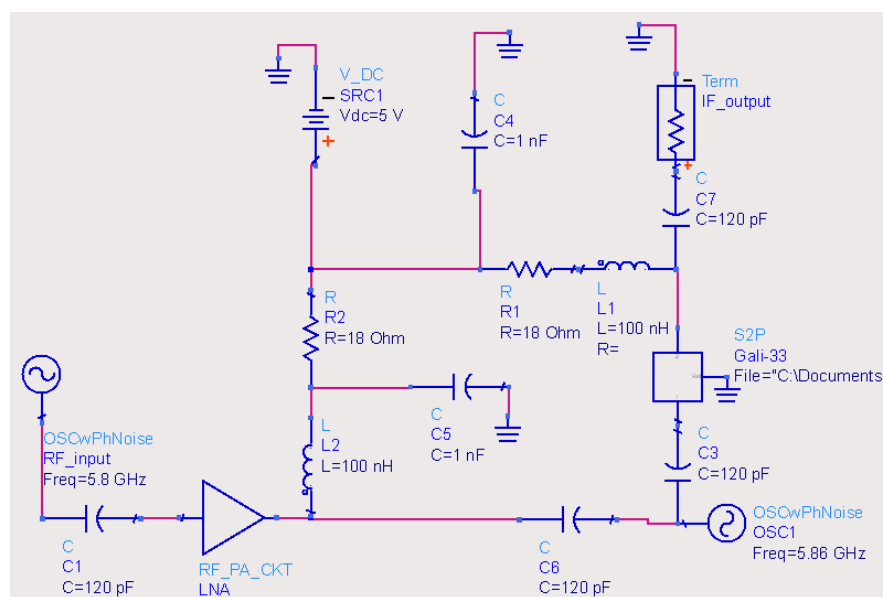


Figure 6-8: Schematics of the Downconverter

After making the schematics, the layout of the circuit was designed on Protel Software. The figure 6-9 shows the layout of the downconverter.

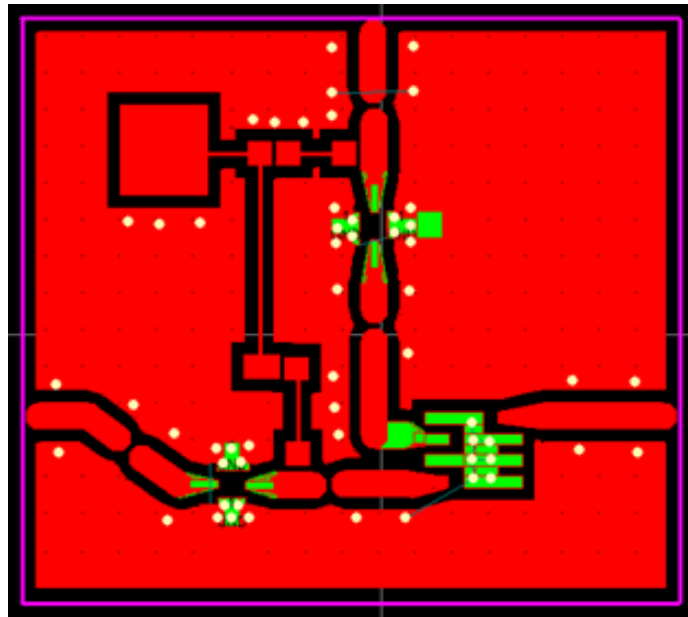


Figure 6-9: Layout of the Downconverter PCB

After fabrication, the downconverter PCB was placed in a microwave housing made out of aluminium. The design and construction of the microwave housing is discussed in the following chapter. Figure 6-10 shows the fabricated downconverter.

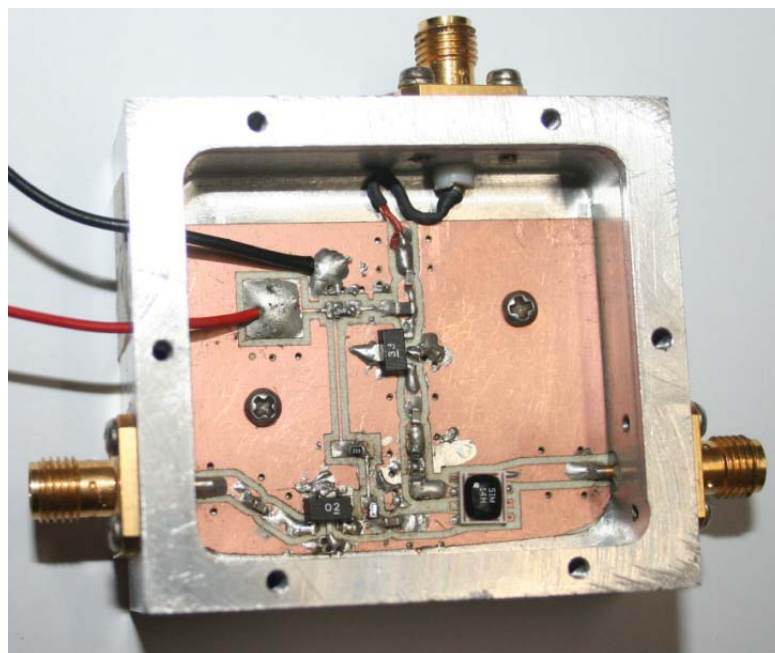


Figure 6-10: Fabricated Downconverter PCB

6.6. Results of the Downconverter

The downconverter is designed to operate at an RF frequency of 5.8 GHz. The power level of this RF signal for the optimum performance of the downconverter is -30 dBm. The LO frequency is 5.86 GHz to obtain an IF of 60 MHz. The drive power level of the LO affects the overall gain of the module. The Table 6-3 represents the overall gain vs. the LO drive power relation.

Table 6-3: Overall Gain vs. the LO Drive power relation

LO Power Level (dBm)	Overall Gain (dB)
7	6
8	14
9	23
10	24
11	25
12	25.3

From the test results it is found out that the optimum LO level is 10 dBm. Increasing LO power beyond this level compresses the mixer.

The following results have been obtained through testing.

Gain: 24 dB

Noise Figure: 2.5 dB

RF VSWR: 1.5

LO VSWR: 2.3

P1dB IF stage: 13 dBm

The downconverting module operates at 5 volts with 70 mA of current supply. Figure 6-11 shows the IF output of the downconverting module. The result has been taken using a spectrum analyzer. The graph shows the IF achieved is 60 MHz and the power level of the IF is -16.22 dBm.

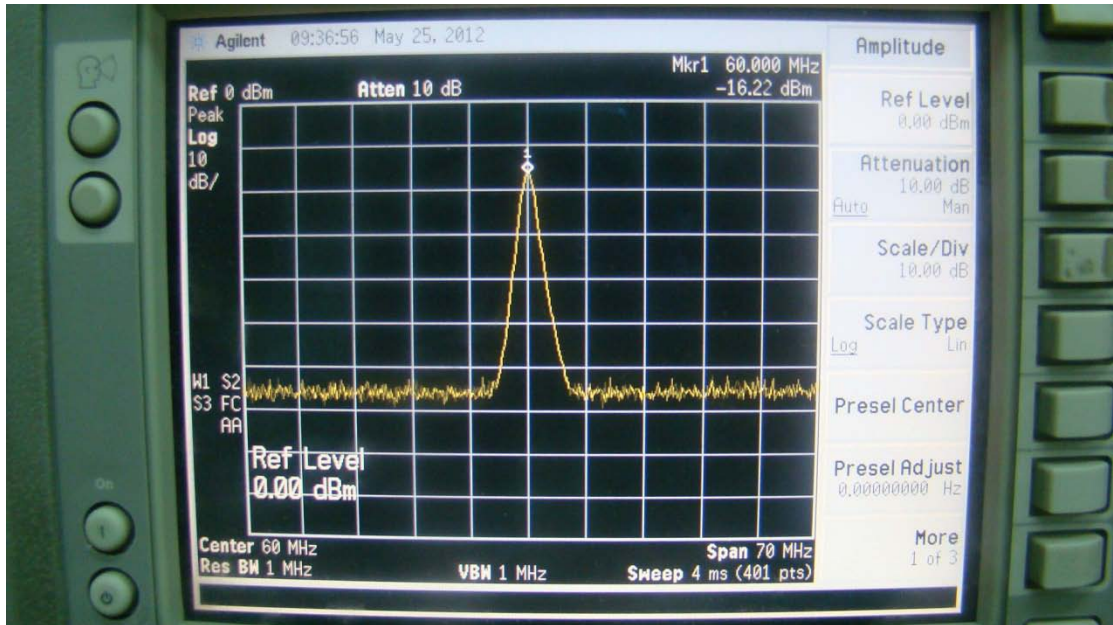


Figure 6-11: IF Output

As mentioned above, the RF VSWR is measured to be 1.54. Figure 6-12 shows the VSWR graph.

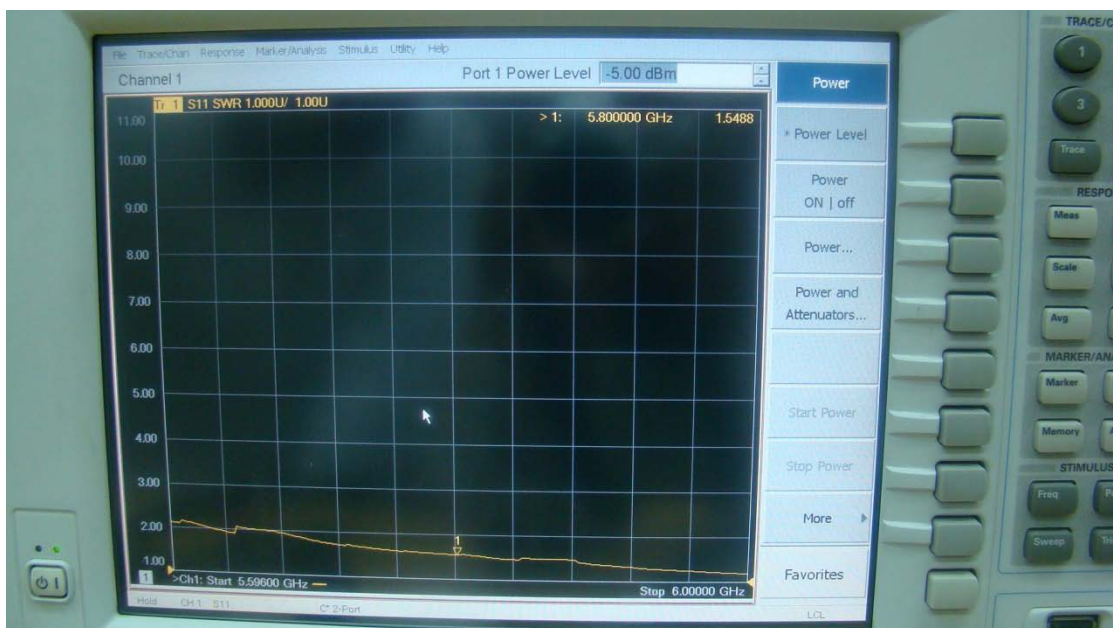


Figure 6-12: RF VSWR

The VSWR of the LO is measured to be 2.3 at a frequency of 5.8 GHz. Figure 6-13 shows the LO VSWR.

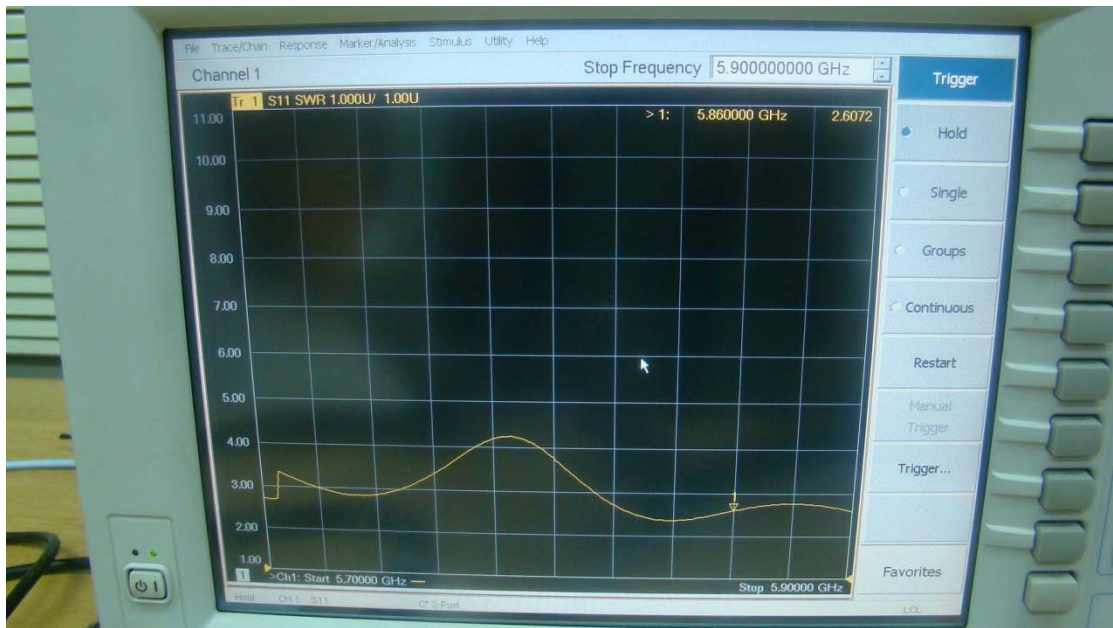


Figure 6-13: LO VSWR

The Figure 6-14 shows the setup for measuring the VSWR. At one port, the probe of the measuring instrument is connected, whereas the other two ports are terminated by means of terminations of 50 Ohms.



Figure 6-14: Setup for Measuring VSWR

The figure 6-15 shows the setup for measuring the Intermediate Frequency.

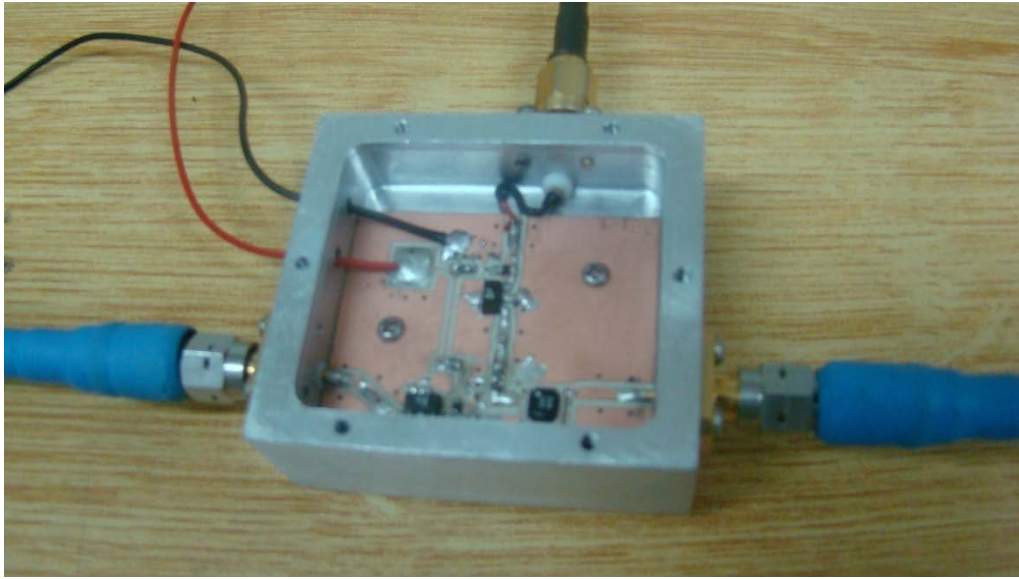


Figure 6-15: Setup for Measuring IF

MICROWAVE HOUSING

The housing designed for microwave circuits as well as that for integrated circuits and Monolithic Microwave Integrated Circuits (MMICs) is very important in the sense that unsuitable dimensions can deteriorate the working and performance of very carefully designed and fabricated circuits and subsystems considerably [11].

The main purpose of the housing is to provide mechanical strength, electric shielding and heat sinking in the case of high power applications. May it be a mixer, an amplifier or a filter, the circuit is usually put into a housing, which is cast or milled from aluminium with connectors attached to the walls of the housing and their pins soldered onto the appropriate microstrip line of the circuit. The connectors can be of type N, SMA or special SMA for mm-wave applications.

A microwave housing with a lid on it forms a cavity and thus exhibits resonance. When the microstrip circuit is mounted into the housing, then this assembly can be thought of as a dielectrically loaded cavity resonator. The frequently faced problem is that the lowest order cavity mode sets a limitation on the maximum frequency for satisfactory operation of the microstrip circuit.

The housing is designed so that the resonating frequency, at which the fundamental cavity mode of the housing occurs, is nowhere near the resonating frequency of the microstrip circuit to be accommodated in the housing. Clearly, if a 5.8 GHz down-converter is accommodated into a housing whose fundamental cavity mode is near 5.8 GHz, then the microstrip down-converter circuit will not work properly. There is a tendency of the lowest order cavity mode to couple to the microstrip circuit with considerable performance deterioration.

The dielectrically loaded housing can be thought of as a lumped circuit LC resonator with the resonance frequency, inductance and capacitance given by the following formulas [12]:

$$f_{101} = \frac{\frac{15}{w} \sqrt{1 + \left(\frac{w}{l}\right)^2}}{\sqrt{\epsilon_r}} \quad (7.1)$$

$$L = \pi \frac{wh}{l \left[1 + \left(\frac{w}{l}\right)^2 \right]} \quad (7.2)$$

$$C = 3.59 \epsilon_r \frac{wl}{h} \quad (7.3)$$

where,

l = length of the housing

w = width of the housing

h = height of the housing

Figures 7-1 and 7-2 show the design of the Microwave Housing in AutoCAD and the isometric view of the housing respectively. The Microwave Housing has been built out of aluminium. The Housing was built using a CNC machine to cater for precision. The downconverter PCB was then housed and adjusted inside Microwave Housing with the help of screws. The adjustment of the PCB in the Microwave Housing has already been discussed and shown in chapter 6.

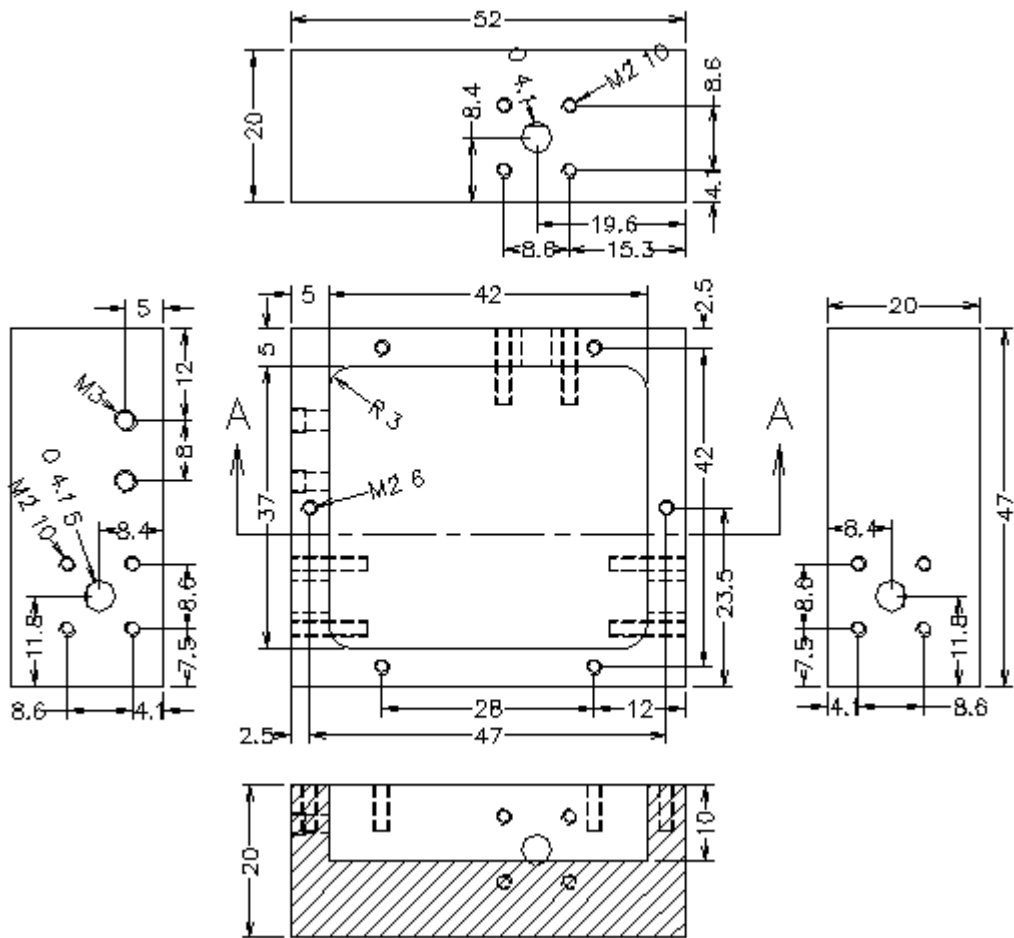


Figure 7-1: Design of Microwave Housing in AutoCAD

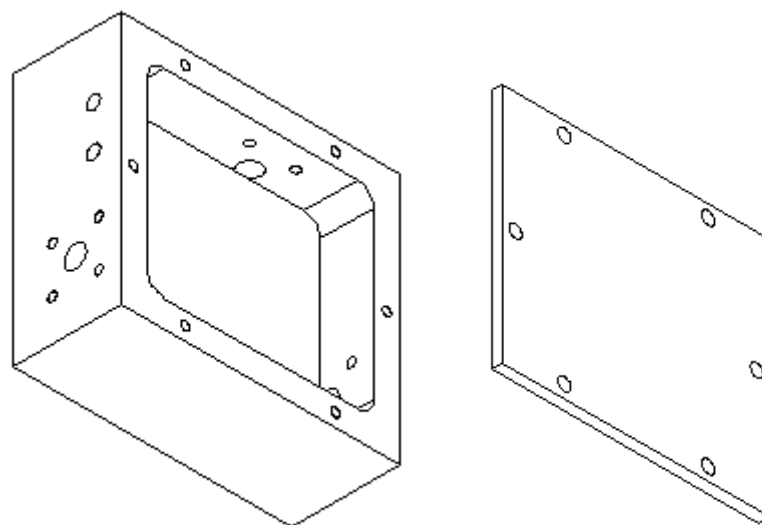


Figure 7-2: Isometric View of Microwave Housing

Figure 7-3 shows the fabricated Microwave housing along with the connectors.

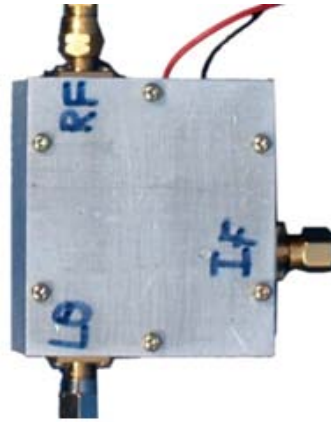


Figure 7-3: Fabricated Microwave Housing

CONTROL CIRCUITRY

8.1. Overview

PIN diode is a device whose impedance at microwave frequencies is controlled by its DC excitation. PIN diodes are unique in their ability to control large amounts of RF power with much lower levels of DC.

PIN diode is a current controlled device. It can be thought of as a current controlled resistor at microwave frequencies. In the PIN diodes, a very high resistive intrinsic I region is sandwiched between P-type and N-type regions. When a PIN diode is forward biased, the holes and electrons are injected into the “I” region from the P-type and N-type regions. These charges do not immediately annihilate each other rather they stay alive for an average time called the carrier life time. This results into an average stored charge, which lowers the effective resistance of the “I” region to a value R_s [13]. Figure 8-1 shows the electrical equivalent model of a forward biased PIN diode.

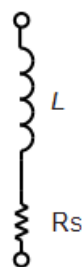


Figure 8-1: Forward Biased Model of PIN Diode

When the PIN diode is reverse biased, there is no stored charge in the I region and the diode appears as capacitor C_T shunted by a parallel resistance R_P . Figure 8-2 shows the equivalent model of a reverse biased PIN diode.

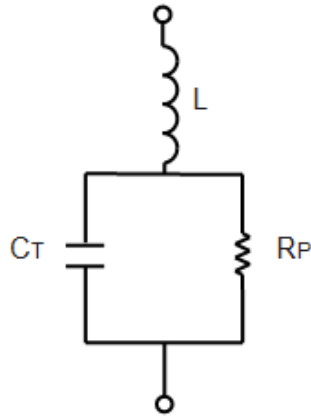


Figure 8-2: Reverse Biased Model of PIN Diode

8.2. Control Signals

The control circuitry generates four signals to control the phase shifting switches. All the four signals are generated using the same oscillator so the four signals are synchronized. The four signals can be given a given a delay relative to each of the using the DIP switches as explained in the following paragraphs. The time delay has a resolution of 4 bits. So, a total of sixteen delay combinations are possible. Change in the state of a single bit produces a delay of 2 microseconds for one control signal relative to the others.

The pulses are generated using the microcontrollers. ATMEGA 16 microcontrollers of the AVR series have been used to generate the control signals. The microcontroller timers are used to generate pulses for driving the PIN diodes. The timers are set in the “restart on compare match mode”. In this mode, the timer restarts every time it reaches a defined value and inverts the output on the output pin, hence creating the output pulses.

DIP switches are attached to the ports of the microcontroller to set the value of the delay between each of the pulses. The controller reads the value of the delay at the

start up and then starts generating pulses according to the delays defined by the switches.

Two microcontrollers have been used to generate the pulses as the number of timers in one controller is three and four timers are needed to generate four independent pulses driven by the same oscillator. The master microcontroller generates two of the pulses. It also controls the clock of the second microcontroller. It starts three of its timers according to the values of the switches and then sends the signal to the second controller after the delay. The second microcontroller starts generating its output pulses as soon as it receives a signal from the first microcontroller.

Figure 8-3 shows the block diagram of the Control circuitry.

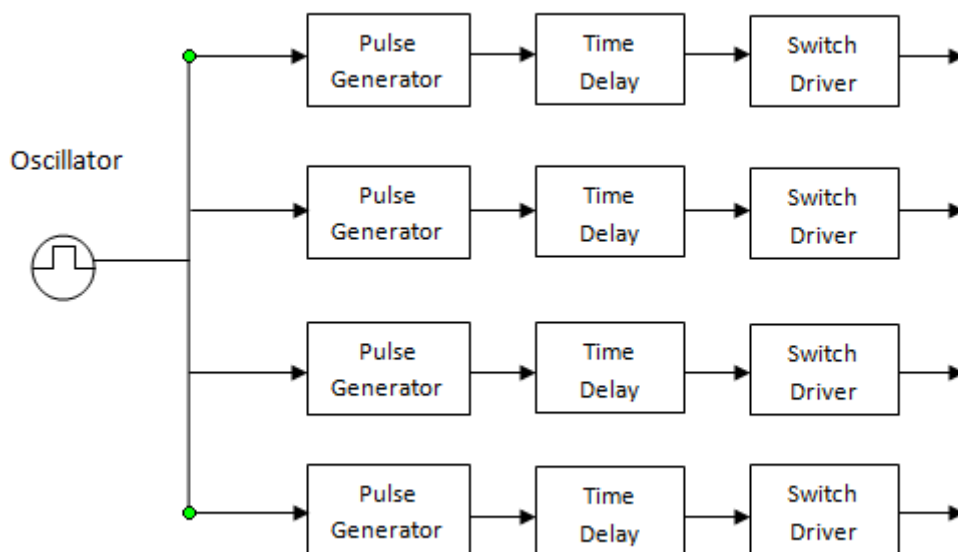


Figure 8-3: Block Diagram of Control Circuitry

The circuit of the pulse generator was simulated in the Proteus Software and the results were verified using the Digital Oscilloscope available in the software.

Figure 8-4 shows the circuit diagram of the pulse generator and time delay circuit.

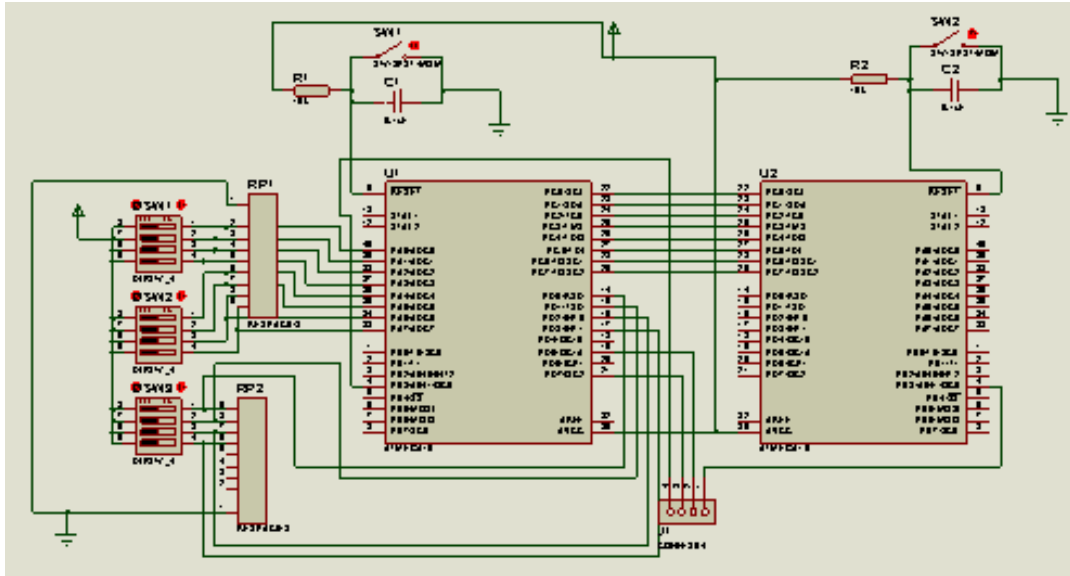


Figure 8-4: Schematics of Pulse Generator and Time Delay Circuit

The output of the pulse generator and time delay circuit are 4 waveforms of the same frequency but with variable relative delay as shown in figure 8-5. The delay between the waveforms is progressive which means that if the delay between first two waveforms is 2 microseconds, then the delay between the first and third waveforms will be 4 microseconds or greater than that, but not less than 2 microseconds.

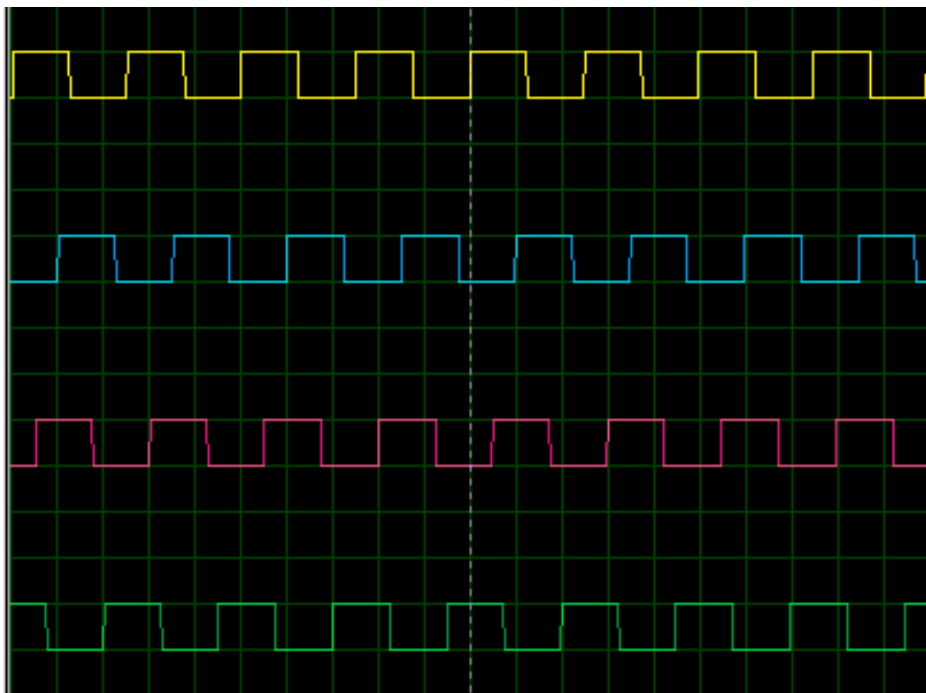


Figure 8-5: Output of Pulse Generator and Time Delay Circuit

8.3. PIN Diode Driver

Every PIN diode in a switching circuit is accompanied by a PIN diode driver that provides a controlled forward bias current, a reverse bias voltage and the activating interface between the control signal and the PIN diode [14].

The designed PIN diode driver supports switching speeds up to 100 MHz. The driver has been designed using transistors and passive components. As the HPND 4028 PIN diodes require a forward biasing current of 5 mA, so the driver circuit outputs a current a current of 5 mA when a positive signal is applied to its input. Figure 8-6 shows the schematic of the PIN diode driver circuit in Proteus Software.

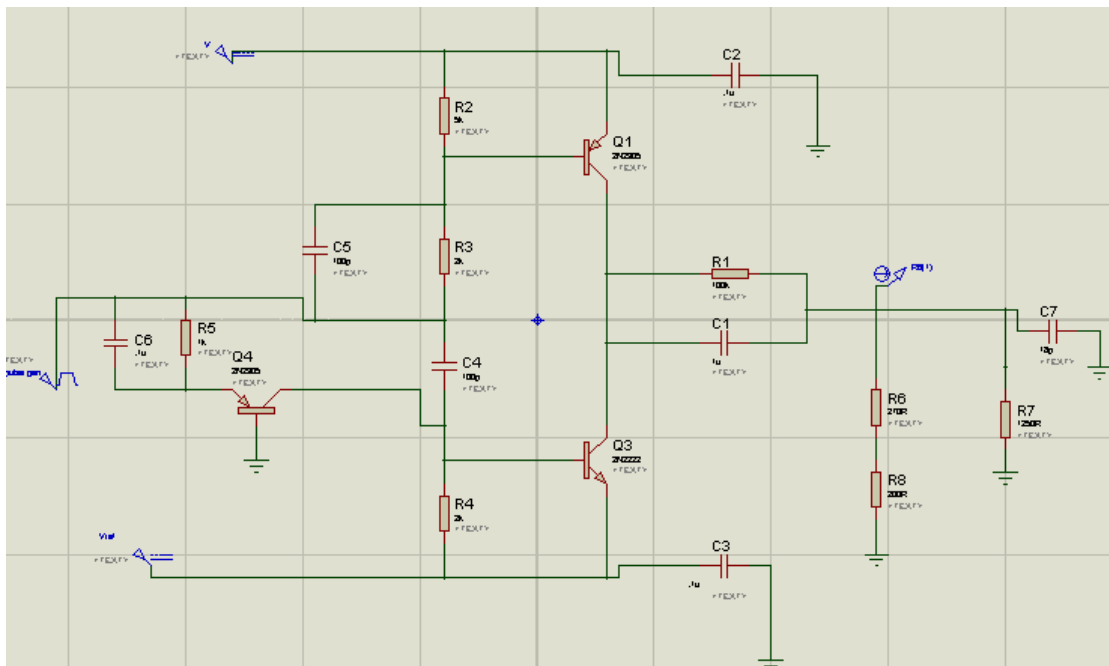


Figure 8-6: Schematic of PIN Diode Driver

BEAMFORMING / BEAM STEERING RESULTS

The results of the project have been obtained from the anechoic chamber. The following picture shows the complete RF front end.



Figure 9-1: Complete Beamformer Structure

Figure 9-2 shows that the main lobe of the beam is at 0 degrees.

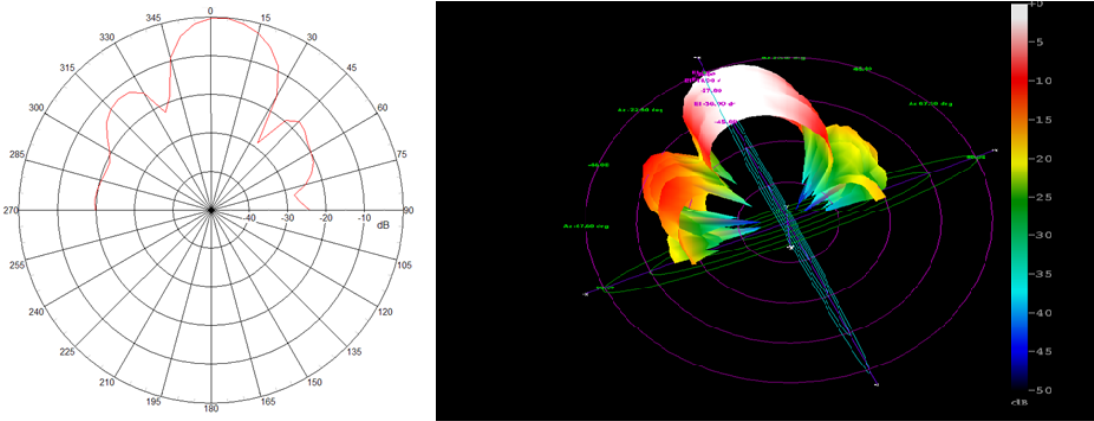


Figure 9-2: Beam at 0 Degrees

Figure 9-3 shows the main lobe of the beam steered at 15 degrees. This was achieved by properly adjusting the time delay of the four control signals discussed in chapter 8.

Figure 9-3 shows that the side lobes are very much suppressed as compared to the main lobe.

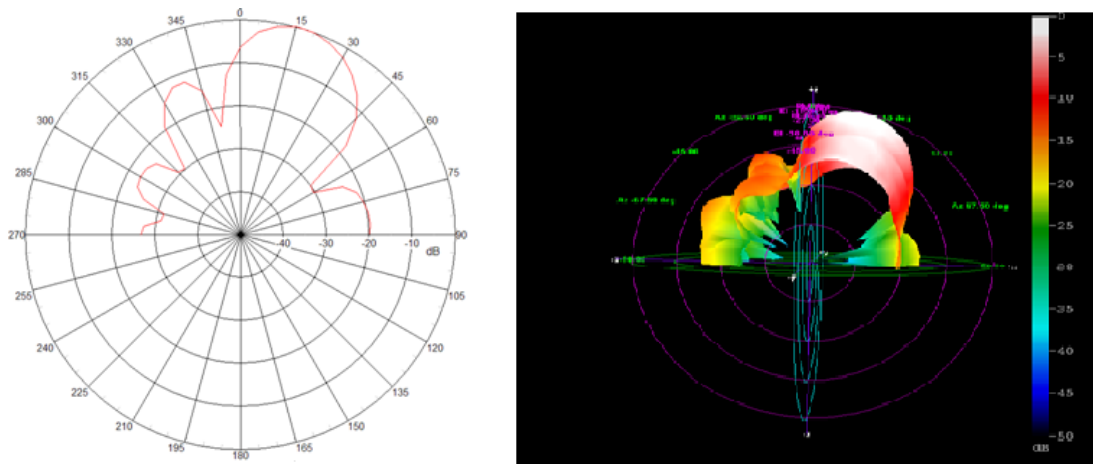


Figure 9-3: Beam Steered at 15 Degrees

Figure 9-4 shows the beam steered at -15 degrees. This result was also achieved by properly adjusting the time delay of the control signals.

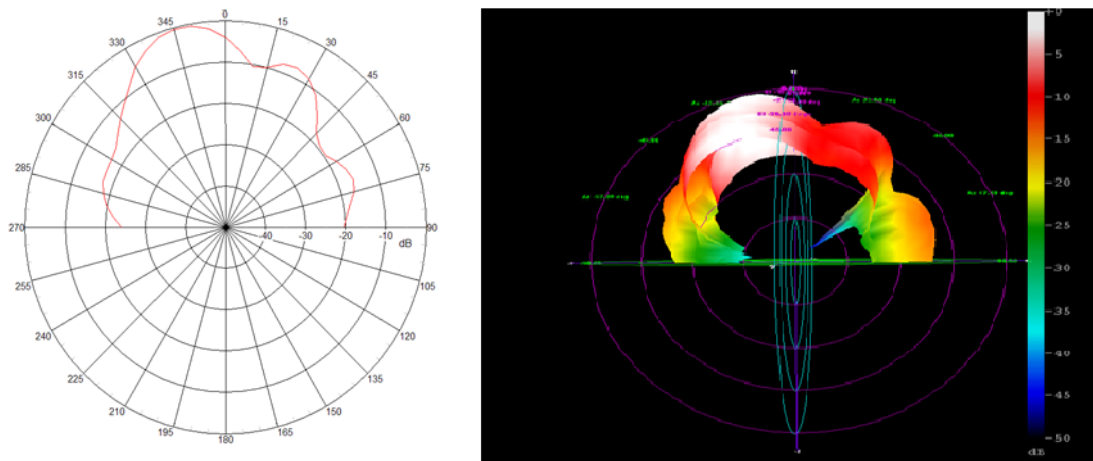


Figure 9-4: Beam Steered at -15 Degrees

Figure 9-5 shows the patterns of the beam steered at 40 degrees. The figure shows that the main lobe of the beam is at 40 degrees and the side lobes are very less as compared to the main lobe.

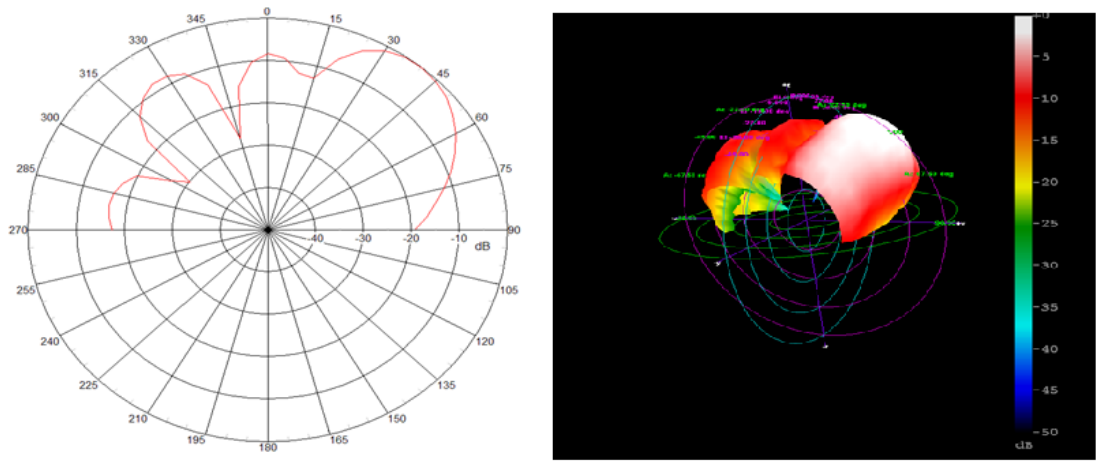


Figure 9-5: Beam Steered at 40 Degrees

CONCLUSION

In this report, the complete background, construction, and the results and analysis of a Microwave Sampling Beamformer had been presented and discussed. A phase shift of 80 degrees has been achieved using this design. The structure is able to steer the beam from -40 degrees to 40 degrees. The design can be enhanced further to incorporate the Direction of Arrival (DOA) algorithms. Incorporating the DOA algorithms into the structure will make the system autonomous which will be able to sense the direction of maximum signal and then adjust the weights properly to steer the beam at the desired angle.

APPENDICES

APPENDIX A

CODE FOR FIRST MICROCONTROLLER

```
int main()

{
    OCR0 = 0x04;
    DDRB = 0xff;
    DDRD = 0xff;
    OCR2 = 0x04;
    OCR1A = 0x04;
    OCR1B = 0x04;
    TCCR1A= 0b01000000;
    DDRA = 0x00;
    DDRB = 0xff;
    DDRC = 0xff;
    w = PINA&0b00001111;
    y = PINA&0b11110000;
    y = y>>4;
    z = PIND&0b00001111;
    a=w;
    b=8+y;
    c=z;
    TCCR0 = 0b00011001;
    for(unsigned char x=0;x<a;x++);
    TCCR2 = 0b00011001;
    for(unsigned char x=0;x<b;x++);
    TCCR1B= 0b00001001;
    for(unsigned char x=0;x<c;x++);
    PORTC = 0xff;
}
```

APPENDIX B

CODE FOR SECOND MICROCONTROLLER

```
#include<avr/io.h>

int main()
{

    OCRO =    0x04;
    DDRB =    0xff;
    DDRD =    0xff;
    DDRA =    0x00;
    DDRB =    0xff;
    DDRC =    0x00;

    while(PINC!=0xff);

    TCCR0 =    0b00011001;

    while(1);

}
```

BIBLIOGRAPHY

BIBLIOGRAPHY

- [1] R.E. Collin, *Foundation for Microwave Engineering*. London McGraw-Hill, 1996.
- [2] U. Rohde, D. Newkirk, *RF Circuit Design for Wireless Applications*, 2000.
- [3] Balanis, Constatine A. *Antenna Theory: Analysis and Design*. 2nd Edition. Singapore: John Willey & Sons, Inc., 2005.
- [4] P.Vizmuller, *RF Design Guide*, 1st ed. Artech House, 685. Canon Street Norwood MA 02062, 1995.
- [5] E.J. Wilkinson, "An N-way Power Divider", *IRE Trans. on Microwave Theory and Techniques*, vol. 8, p. 116-118, Jan. 1960.
- [6] Pozar, David M. *Microwave Engineering*. 3rd Edition. Jonh Wiley & Sons, 1997.
- [7] S. Farzaneh and A.R.Sebak, "Microwave Sampling Beamformer – Prototype verification and Switch Design", *IEEE Trans. Microw. Theory Tech.*, vol. 57, no. 1, pp. 36-44, January 2009
- [8] Henderson, B. C., "Predicting Intermodulation Suppression in Double-Balanced Mixers," Watkins-Johnson Company Technical Notes. Vol. 10, No. 4, July/August 1983.
- [9] Marki, F.A., "Miniature Image Reject Mixers And Their Use In Low-noise Front-ends In Conjunction With GaAs FET Amplifiers," *Circuits, Systems and Computers*, 1977. Conference record. 1977 11th Asilomar Conference, vol., no., pp. 159-162, 7-9 Nov 1977.
- [10] Ludwig. R., Bretchko. P, *RF Circuit Design: Theory and Applications*. Upper Saddle River, NJ, Prentice Hall, 2000.
- [11] Ellis Honwood. Limited, L.A. Trinogga, Guo Kaizhou, I.C. Hunter, *Practical Microstrip Circuit Design*, 1991.

- [12] L. Besser and R. Gilmore, *Practical RF Circuit Design for Modern Wireless Systems*. Volume 1, Boston: Artech House, 2003.
- [13] *Radiotron Designer's Handbook*, 3rd ed, edited by. F. Langford Smith, published by RCA Manufacturing Company, Harrison, N. J, 1942.
- [14] W. Alan Davis and Krishna Agarwal, *Radio Frequency Circuit. Design*, John Wiley & Sons, 2003.